AD-A053 030 MASSACHUSETTS INST OF TECH CAMBRIDGE DEPT OF MECHANI--ETC F/G 13/7
HYDRAULIC SIGNAL-PROCESSING AMPLIFIER PERFORMANCE IN POSITION C--ETC(U)
DEC 77 D LEE, D N WORMLEY DAAG29-74-C-0191

UNCLASSIFIED HDL-CR-77-191-1 NL

| OF |
AD A053030

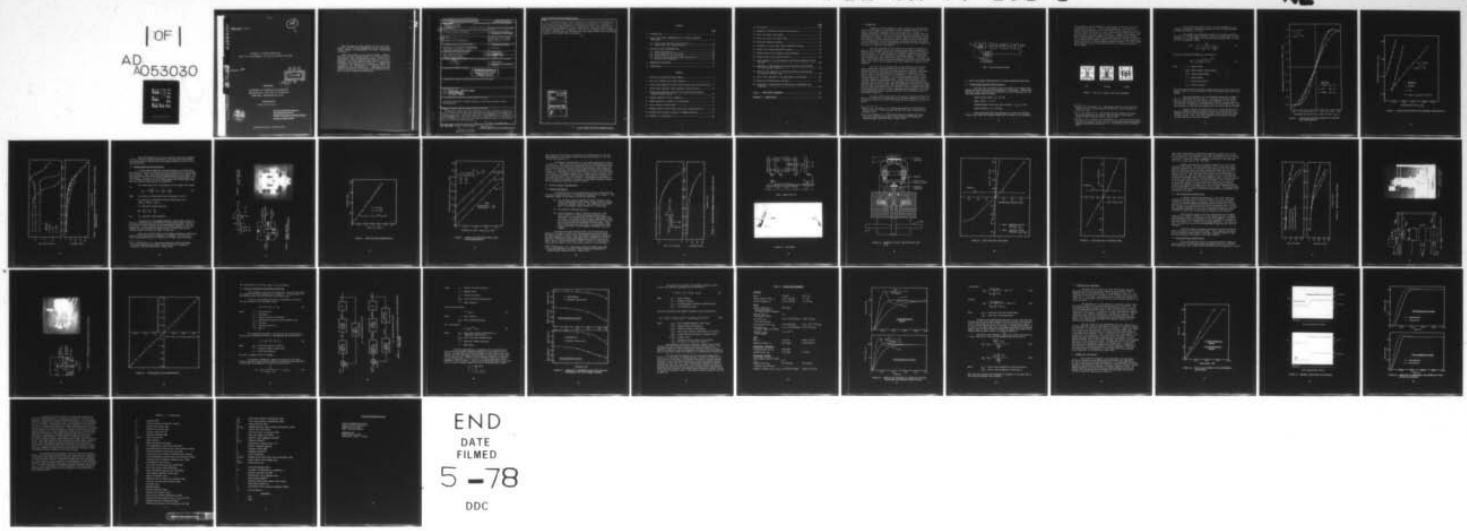

END
DATE FILMED
5 -78
DDC

HDL-CR-77-191-1

12

HYDRAULIC SIGNAL-PROCESSING AMPLIFIER PERFORMANCE IN POSITION CONTROL SYSTEMS

DECEMBER 1977

Prepared by

DEPARTMENT OF MECHANICAL ENGINEERING
MASSACHUSETTS INSTITUTE OF TECHNOLOGY
CAMBRIDGE, MASSACHUSETTS 02139

Under Contract

DAAG-29-74-C-0191

U.S. Army Materiel Development and Readiness Command
HARRY DIAMOND LABORATORIES
Adelphi, Maryland 20783

The findings of this report are not to be construed as an official Department of the Army position, unless so designated by other authorized documents.

When this report is no longer needed, Department of the Army organizations will destroy it in accordance with the procedure given in AR 380-5. Navy and Air Force elements will destroy it in accordance with applicable directives. Department of Defense contractors will destroy the report according to the requirements of section 14 of the Industrial Security Manual for Safeguarding Classified Information. All others will return the report to Harry Diamond Laboratories.

SECURITY CLASSIFICATION OF THIS PAGE *(When Data Entered)*

REPORT DOCUMENTATION PAGE

READ INSTRUCTIONS BEFORE COMPLETING FORM

1. REPORT NUMBER: HDL-CR-77-191-1
2. GOVT ACCESSION NO.
3. RECIPIENT'S CATALOG NUMBER

4. TITLE *(and Subtitle)*: Hydraulic Signal-Processing Amplifier Performance in Position Control Systems.

5. TYPE OF REPORT & PERIOD COVERED: Contractor Report.

6. PERFORMING ORG. REPORT NUMBER

7. AUTHOR(s): David Lee, David N. Wormley

8. CONTRACT OR GRANT NUMBER(s): DAAG-29-74-C-0191

9. PERFORMING ORGANIZATION NAME AND ADDRESS
Department of Mechanical Engineering
Massachusetts Institute of Technology
Cambridge, Massachusetts 02139

10. PROGRAM ELEMENT, PROJECT, TASK AREA & WORK UNIT NUMBERS: 6.11.02.A

11. CONTROLLING OFFICE NAME AND ADDRESS
Harry Diamond Laboratories
2800 Powder Mill Road
Adelphi, Maryland 20783

12. REPORT DATE: December 1977

13. NUMBER OF PAGES: 43

14. MONITORING AGENCY NAME & ADDRESS *(if different from Controlling Office)*

15. SECURITY CLASS. *(of this report)*: UNCLASSIFIED

15a. DECLASSIFICATION/DOWNGRADING SCHEDULE

16. DISTRIBUTION STATEMENT *(of this Report)*

DISTRIBUTION STATEMENT A
Approved for public release;
Distribution Unlimited

17. DISTRIBUTION STATEMENT *(of the abstract entered in Block 20, if different from Report)*

18. SUPPLEMENTARY NOTES
DRCMS Code: 611102.11.71200
DA 1T161102A33B
HDL Proj: 302431

19. KEY WORDS *(Continue on reverse side if necessary and identify by block number)*
Proportional Amplifier, Summing Amplifier, Servovalve, Position Control Servomechanism

20. ABSTRACT *(Continue on reverse side if necessary and identify by block number)*

Summing and proportional gain amplifiers for use in hydraulic closed-loop position control systems have been developed and their static and dynamic characteristics measured. Amplifiers constructed using ~~HDL~~ laminar flow laminate designs ~~311005~~ with 0.5 mm nozzle width and an aspect ratio of 2.0 exhibited frequency responses with less than 3 dB decay and 90 deg phase shift at 300 Hz when operated at 110 kPa supply pressure.

Con't. on other side

DD FORM 1 JAN 73 1473 EDITION OF 1 NOV 65 IS OBSOLETE

SECURITY CLASSIFICATION OF THIS PAGE *(When Data Entered)*

220022

20

A closed-loop position control system for a load mass has been developed and tested using the summing and proportional gain amplifier, a position-to-fluid pressure feedback transducer, a hydraulic actuator, and a two-stage commercial servovalve modified to accept fluid inputs. Tests performed on the servosystem demonstrated a response to position step command, with no overshoot, in 38 ms. Analysis and test data show that the primary element limiting dynamic response is the fluidic input servovalve.

CONTENTS

		Page
1.	INTRODUCTION	5
2.	STATIC AND DYNAMIC CHARACTERISTICS OF SIGNAL PROCESSING AMPLIFIERS	6
	2.1 Single-Stage Amplifier Characteristics	6
	2.2 Summing Amplifier Characteristics	12
3.	POSITION CONTROL SERVOMECHANISM	16
	3.1 General Description	16
	3.2 Fluid Controlled Position Servo	22
	3.3 Electrohydraulic Position Servo	22
	3.4 Position Servosystem Linear Model Description	27
	3.5 Measured Servo Responses	35
4.	SUMMARY AND CONCLUSIONS	35
5.	DISTRIBUTION	43

FIGURES

1	Positional servosystem block diagram	6
2	The 2-2B, 231004A, and 311005 laminates	7
3	Single-stage amplifier blocked load pressure gain characteristics	9
4	Single-stage amplifier input impedance characteristics	10
5	Single-stage amplifier blocked load pressure gain frequency response characteristics	11
6	Summing amplifier circuit schematic	13
7	Summing amplifier schematic and photograph	13
8	Input resistor characteristics	14
9	Summing amplifier multi-input static gain characteristics	15
10	Blocked load frequency response of summing amplifier	17
11	Schematic of load setup	18

Page

12 Load setup..... 18

13 Schematic of fluid and electrical input valve..... 19

14 Valve flow gain; fluid input..... 20

15 Valve flow gain; electrical input..... 21

16 Servovalve dynamic response..... 23

17 Schematic of closed-loop fluidic-mechanical system..... 24

18 Closed loop fluidic-mechanical system..... 24

19 Flapper-nozzle valve schematic and photograph..... 25

20 Flapper-nozzle valve characteristics..... 26

21 Block diagram of electromechanical and fluidic-mechanical servo-systems..... 28

22 Comparison of experimental data with analytical approximation for valve dynamic response..... 30

23 Computed step responses of closed-loop position servosystems for selected values of gain..... 33

24 Static load stiffness of the experimental servosystems..... 36

25 Measured servosystem step responses..... 37

26 Comparison of experimental and theoretical servosystem step responses..... 38

TABLE I: SERVOSYSTEM PARAMETERS..... 32

APPENDIX A: NOMENCLATURE..... 41

1. INTRODUCTION

Hydraulic control systems are used extensively in applications where high performance is required in terms of response speed, high force levels, large power-to-weight ratios, and reliability. The performance capability of hydraulic control systems can be extended with the development of effective pure fluid sensing, signal processing, and power amplification elements. The use of a common fluid for both signal processing elements and power modulation/actuation elements and the elimination of electromechanical and electrohydraulic interfaces increases the potential for application of pure fluid-mechanical systems in severe temperature, vibration, or radiation environments.

The work described in this report is one phase of research directed to the development of pure fluid sensing and signal processing elements, as well as power amplification and modulation elements for hydraulic control systems. In previous phases of research, design techniques and fluid elements have been developed for multistage hydraulic fluid amplifiers for pressure, flow, and/or power gain[1]; in addition, a four-way, two-stage fluid input servovalve has been developed to provide the link between signal power levels and the higher power level modulation required for actuators.[2]

The focus of the current work has been directed to two areas. First, summing and signal processing units have been designed, built, and tested, using a new series of fluidic amplifier laminates, HDL design 311005. These units have improved performance in comparison to units cited by Wormley and Wilson[1] and Lee and Wormley.[2] The second area of work has led to the development of a closed-loop position servo, illustrated schematically in figure 1, with a fluid feedback position sensor, a fluidic signal processing amplifier, a fluid input servovalve, and a hydraulic ram with a mass load. The performance of this system has been compared directly with a closed-loop electrohydraulic position servo using the same main stage servovalve, ram, and mass load to illustrate the similarity in overall performance and to identify the areas in which differences in characteristics occur. Section 2 describes the development of the pure fluid summing and signal processing amplifier; the closed-loop servo is described in Section 3.

The test results described in this report have been obtained with Univis J-43 hydraulic oil maintained at an operating temperature of 27° C. The density of the oil is 8.69×10^2 kg/m^3 and the viscosity is 1.88×10^{-2} N-s/m^2.

---

[1] Wormley, D.N. and Wilson, D.R., "Multistage Hydraulic Fluid Amplifier Characteristics," Technical Report HDL-TR-156-1, Harry Diamond Laboratories, 1974.

[2] Lee, D. and Wormley, D.N., "Multistage Hydraulic Summing and Signal Processing Amplifiers and Fluidic Input Servovalve Development," Technical Report HDL-CR-76-223-1, October 1976.

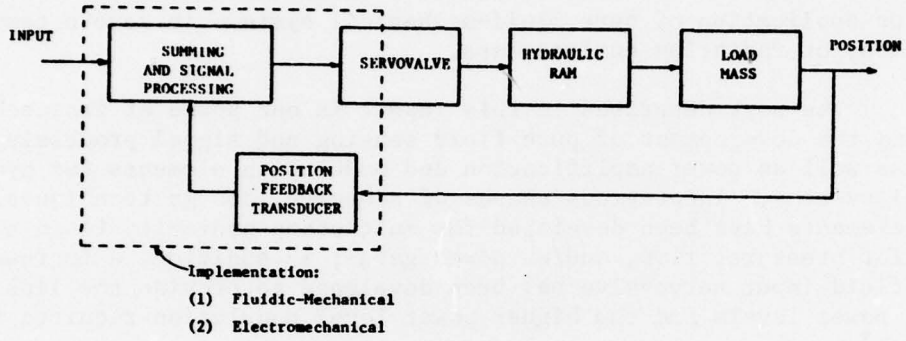

FIGURE 1: POSITIONAL SERVOSYSTEM BLOCK DIAGRAM

2. STATIC AND DYNAMIC CHARACTERISTICS OF SIGNAL PROCESSING AMPLIFIERS

2.1 Single-Stage Amplifier Characteristics

The basis for the position servo controller is a single-stage summing amplifier constructed from laminates of HDL design. Single-stage amplifiers constructed from these laminates have been developed with the following nominal characteristics.

Supply nozzle width: $b_s = 0.5$ mm

Aspect ratio: $\sigma = 2.0$

Nondimensional control port bias pressure: $P_{co}/P_s = 0.05$

Supply pressure: $P_s = 110$ kPa

These amplifiers have been designed to provide the interface between fluid input and feedback signals and the input to the servovalve

as described by Lee and Wormley[2]. A photograph of the three laminates is displayed in figure 2. The laminates represent a succession of designs, beginning with the 2-2B and 231004A, which were used in amplifiers described in References 1 and 2, and then the 311005 laminate, which has been used in the more recent amplifiers. Computer-aided design[3] was used to develop this new laminate to achieve a higher input impedance and a larger bandwidth than the previous laminates. As shown in figure 2, the new design has decreased length in the input and output channels and larger side vents to achieve improved dynamic response. The input channel-jet interaction region has also been altered by increasing the nozzle throat length.

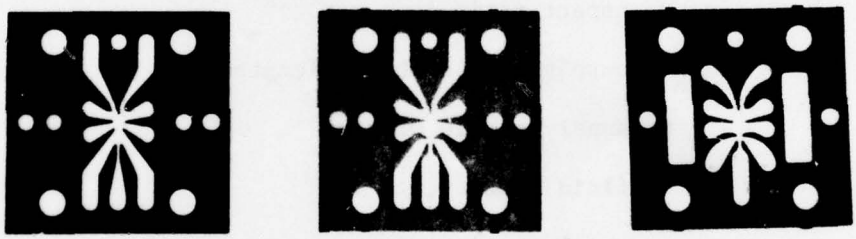

2-2B 231004A 311005

FIGURE 2: THE 2-2B, 231004A, AND 311005 LAMINATES

---

[1] Wormley, D.N. and Wilson, D.R., "Multistage Hydraulic Fluid Amplifier Characteristics," Technical Report HDL-TR-156-1, Harry Diamond Laboratories, 1974.

[2] Lee, D. and Wormley, D.N., "Multistage Hydraulic Summing and Signal Processing Amplifiers and Fluidic Input Servovalve Development," Technical Report HDL-CR-76-223-1, October 1976.

[3] Drzewiecki, T.M., Wormley, D.N. and Manion, F.M., "Computer-Aided Design Procedure for Laminar Fluidic Systems," Trans. ASME, Journal of Dynamic Systems, Measurement and Control, Vol. 97, Series G, No. 4, December 1975.

The blocked load pressure gains, the input impedances, and frequency responses of amplifiers constructed from the three laminates are shown in figures 3, 4, and 5.

The blocked load pressure gain data for the three amplifiers are taken at the same supply pressure. Because of differences in nozzle goemetry, i.e. throat length, the modified Reynolds Number N_R', is different for each amplifier where:

$$N_R' = \frac{N_R}{\left(1 + \frac{1}{\sigma}\right)^2 \left(1 + \frac{X_{th}}{b_s}\right)}, \qquad (1)$$

and where the Reynolds Number N_R is defined as

$$N_R = b_s \left(\frac{\rho}{\mu}\right)\left(\frac{2P_s}{\rho}\right)^{1/2}, \qquad (2)$$

and

σ = aspect ratio,

X_{th} = supply nozzle throat length,

b_s = supply nozzle width,

ρ = fluid density,

μ = absolute viscosity,

P_s = supply pressure.

The three amplifiers have similarly shaped blocked load gain curves with gains at null of 13 for the 2-2B, of 8 for the 231004A, and of 10 for the 311005.

The input impedances for the amplifiers displayed in figure 5 are 5.0×10^9 N-s/m^5 for the 2-2B, 1.7×10^{10} N-s/m^5 for the 231004A, and 1.4×10^{10} N-s/m^5 for the 311005. The impedances for the latter two amplifiers are greater by approximately a factor of three than that for the 2-2B. In addition, the control flow for the 311005 is less than that required for the two other amplifiers at any given control pressure.

Dynamic frequency response data for the three amplifiers displayed in figure 5 shows that 90° phase shift is reached by the 2-2B amplifier at 140 Hz, by the 231004A at about 290 Hz, and by the 311005 at about 340 Hz. Thus, the 311005 amplifier has extended frequency response compared to the other designs.

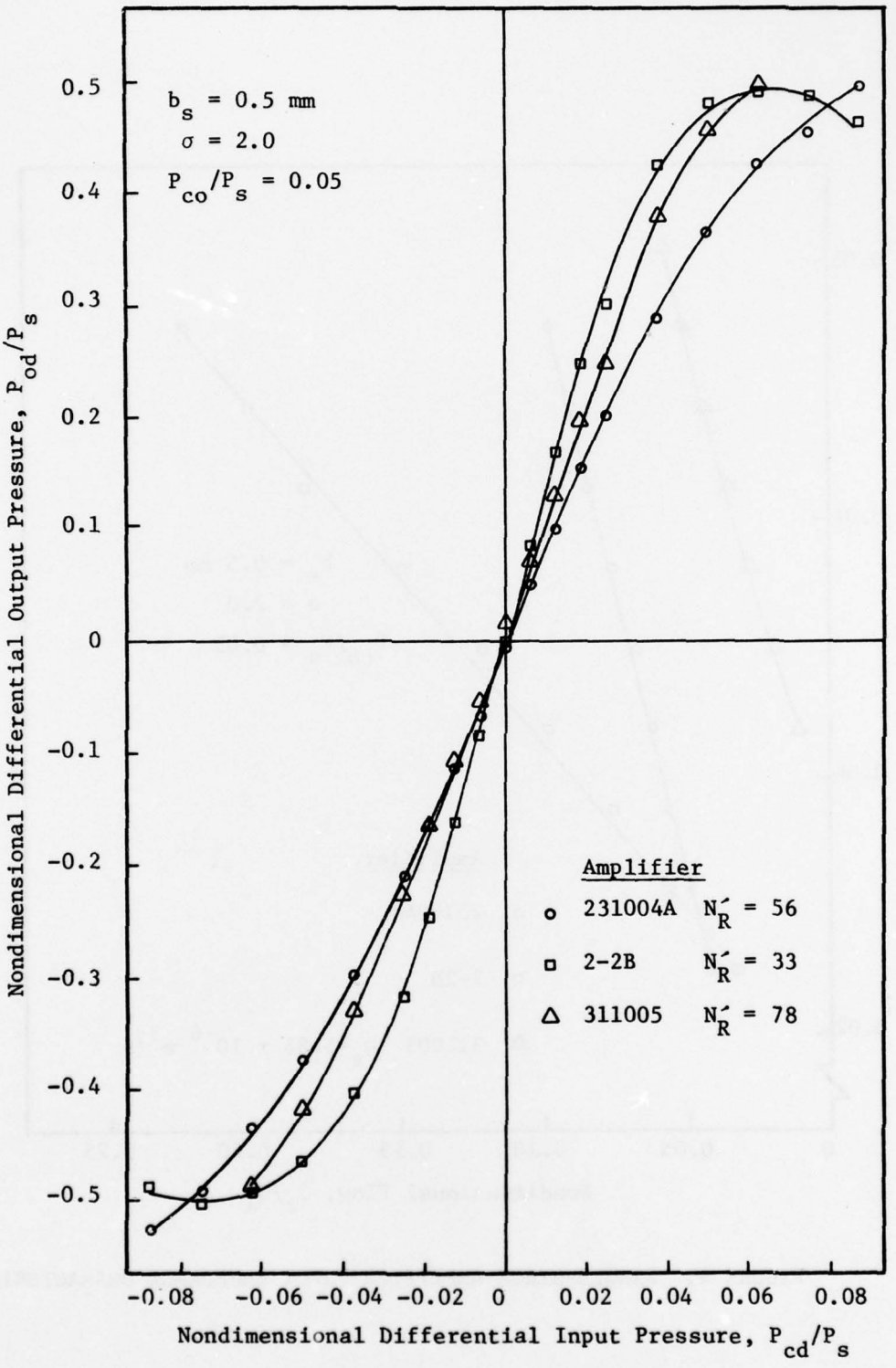

FIGURE 3: SINGLE-STAGE AMPLIFIER BLOCKED LOAD PRESSURE GAIN CHARACTERISTICS

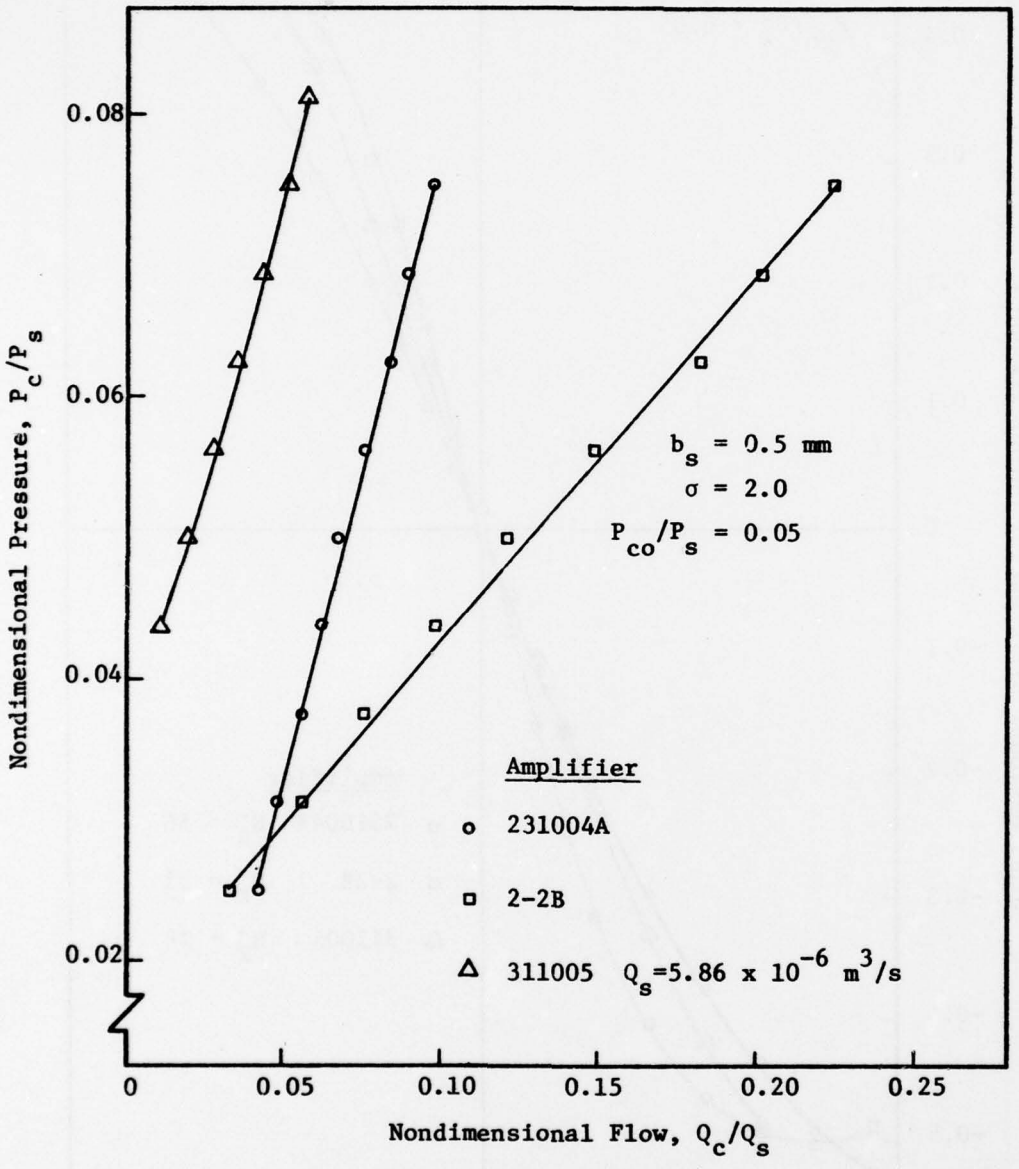

FIGURE 4: SINGLE-STAGE AMPLIFIER INPUT IMPEDANCE CHARACTERISTICS

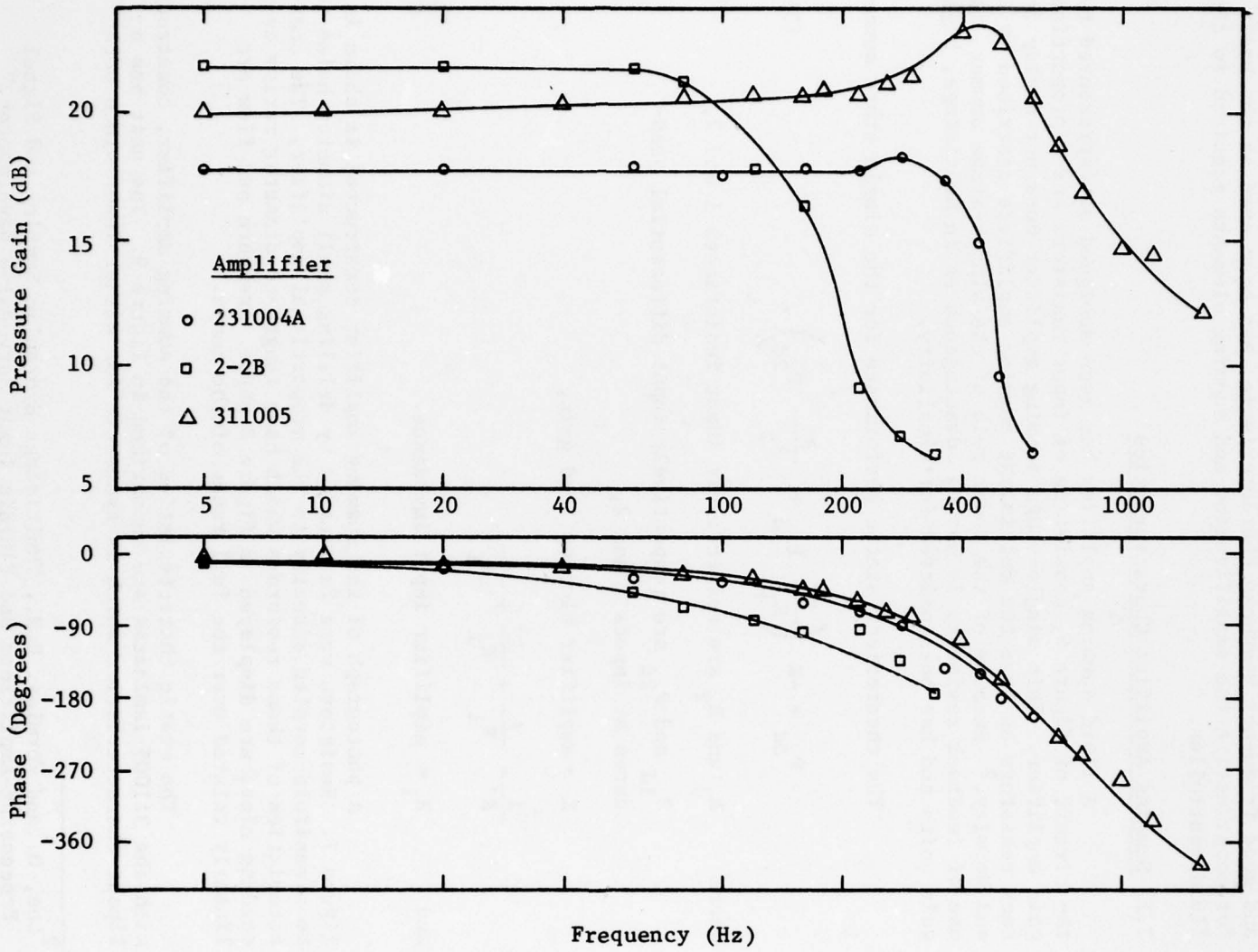

FIGURE 5: SINGLE-STAGE AMPLIFIER BLOCKED LOAD PRESSURE GAIN FREQUENCY RESPONSE CHARACTERISTICS

The 311005 amplifier, with its relatively high input impedance and good frequency response characteristic, has been used as the basis for constructing the amplification and summing elements required in the fluid controller.

2.2 Summing Amplifier Characteristics

A fluid summing amplifier has been designed as represented by the circuit of figure 6, consisting of input resistors and a proportional gain amplifier. This single-stage summing amplifier does not employ feedback resistors as have the multistage summing amplifiers described by Lee and Wormley.[2] Because of the lower gain of the single-stage summer, the use of feedback resistors is not as advantageous as in multistage, high-gain units and has been omitted for simplicity.

The theoretical static performance for the single state summer is

$$P_{od} = -K \left(\frac{R'}{R_1} P_{1d} + \frac{R'}{R_2} P_{2d} \right), \qquad (3)$$

where R_1 and R_2 are respectively input resistances 1 and 2,

P_{1d} and P_{2d} are respectively input differential pressures at inputs 1 and 2,

K = amplifier blocked load gain,

$$\frac{1}{R'} = \frac{1}{R_1} + \frac{1}{R_2} + \frac{1}{R_i},$$

and R_i = amplifier input impedance.

A photograph of the summing amplifier constructed is shown in figure 7. Resistors were fabricated by drilling small diameter holes into a manifold coupled directly to the proportional amplifier. The characteristics of these resistors which have length-to-diameter ratios exceeding nine, are displayed in figure 8 where pressure and flow are linearly related over the full range of the curve.

The static characteristics of the summing amplifier, constructed with the 311005 laminates are summarized in figure 9. The unit has a linear characteristics which is symmetric for either input since both

---

[2] Lee, D. and Wormley, D.N., "Multistage Hydraulic Summing and Signal Processing Amplifiers and Fluidic Input Servovalve Development," Technical Report HDL-CR-76-223-1, October 1976.

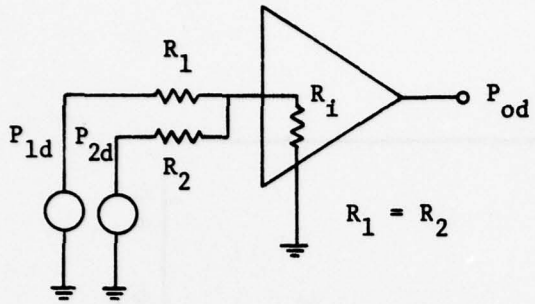

FIGURE 6: SUMMING AMPLIFIER CIRCUIT SCHEMATIC

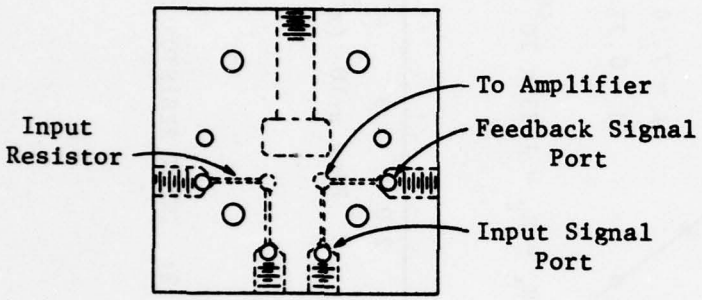

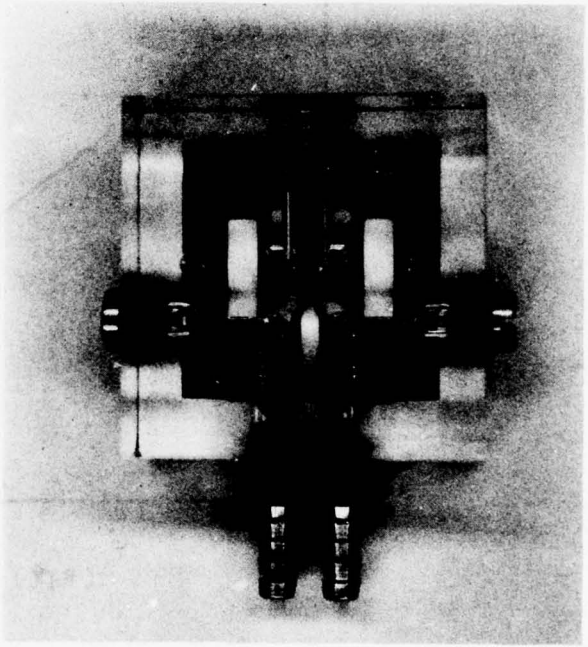

FIGURE 7: SUMMING AMPLIFIER SCHEMATIC AND PHOTOGRAPH

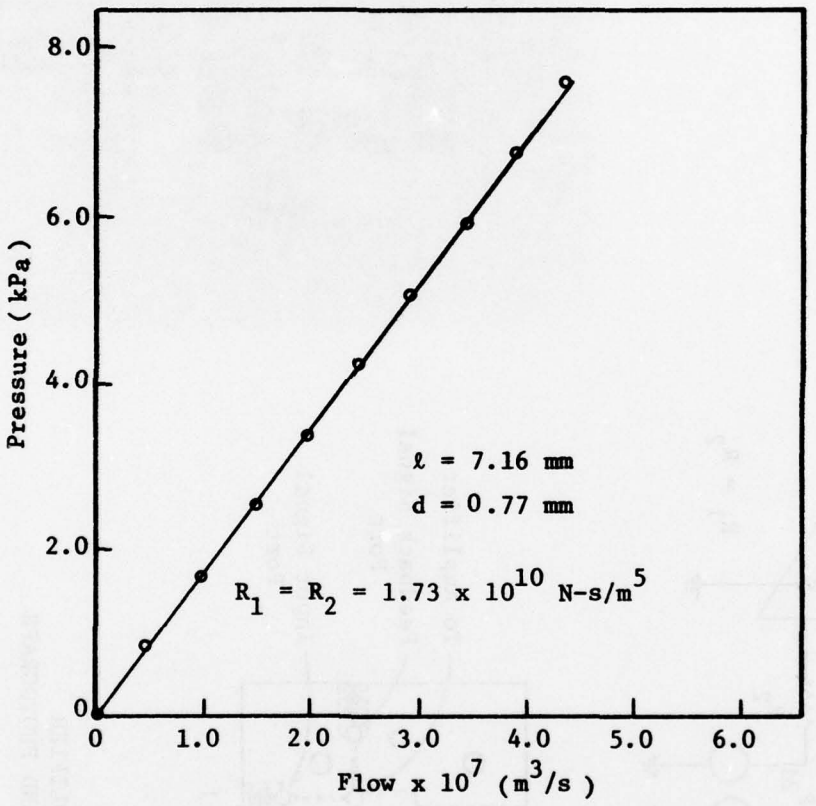

FIGURE 8: INPUT RESISTOR CHARACTERISTICS

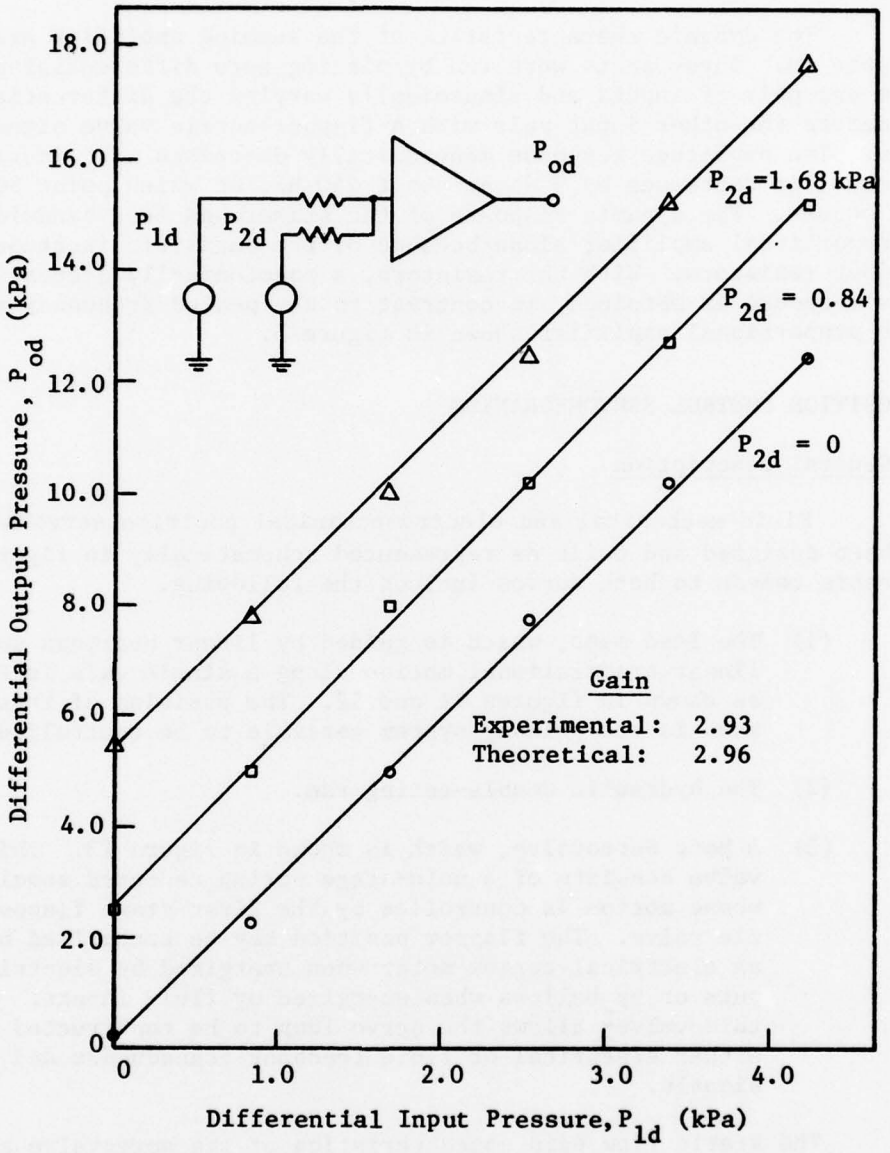

FIGURE 9: SUMMING AMPLIFIER MULTI-INPUT STATIC GAIN CHARACTERISTICS

inputs have the same value of resistance. The measured gain of the summing amplifier is 2.96, which agrees closely with the gain of 2.93 calculated from equation (3).

The dynamic characteristics of the summing amplifier are shown in figure 10. These tests were run by placing zero differential pressure across one pair of inputs and sinusoidally varying the differential pressure across the other input pair with a flapper-nozzle valve signal generator. The amplitude response monotonically decreases with increasing frequency; it decreases by 3 db at about 240 Hz, at which point 90° phase shift occurs. The dynamic response of the summer has less bandwidth than the proportional amplifier alone because of the parasitic inertance in the input resistors. With the resistors, a monotonically decreasing frequency response is obtained, in contrast to the peaked frequency response of the proportional amplifier shown in figure 5.

3. POSITION CONTROL SERVOMECHANISM

3.1 General Description

Fluid-mechanical and electromechanical position servomechanisms have been designed and built as represented schematically in figure 1. The components common to both servos include the following.

(1) The load mass, which is guided by linear bearings so that linear translational motion along a single axis is achieved, as shown in figures 11 and 12. The position of this load mass is the primary system variable to be controlled.

(2) The hydraulic double-acting ram.

(3) A Moog Servovalve, which is shown in figure 13. This valve consists of a main-stage spring centered spool whose motion is controlled by the first-stage flapper-nozzle valve. The flapper position may be controlled by either an electrical torque motor when energized by electrical inputs or by bellows when energized by fluid inputs. Thus, this valve[2] allows the servo loop to be constructed using either electrical or fluid feedback transducers and input signals.

The static flow gain characteristics of the servovalve are summarized in figures 14 and 15 for both fluid and electrical inputs. The data illustrate a nearly linear relationship between both inputs and the corresponding flow output. The fluid input (including the fluidic amplifier, constructed from 311005 laminates specified in section 2), static gain is about 10^4 mm^3/s/kPa for inputs in the 0 to 2 kPa pressure range, and the electric input static gain is about 5 x 10^3 mm^3/s/mA.

---

[2]Lee, D. and Wormley, D.N., "Multistage Hydraulic Summing and Signal Processing Amplifiers and Fluidic Input Servovalve Development," Technical Report HDL-CR-76-223-1, October 1976.

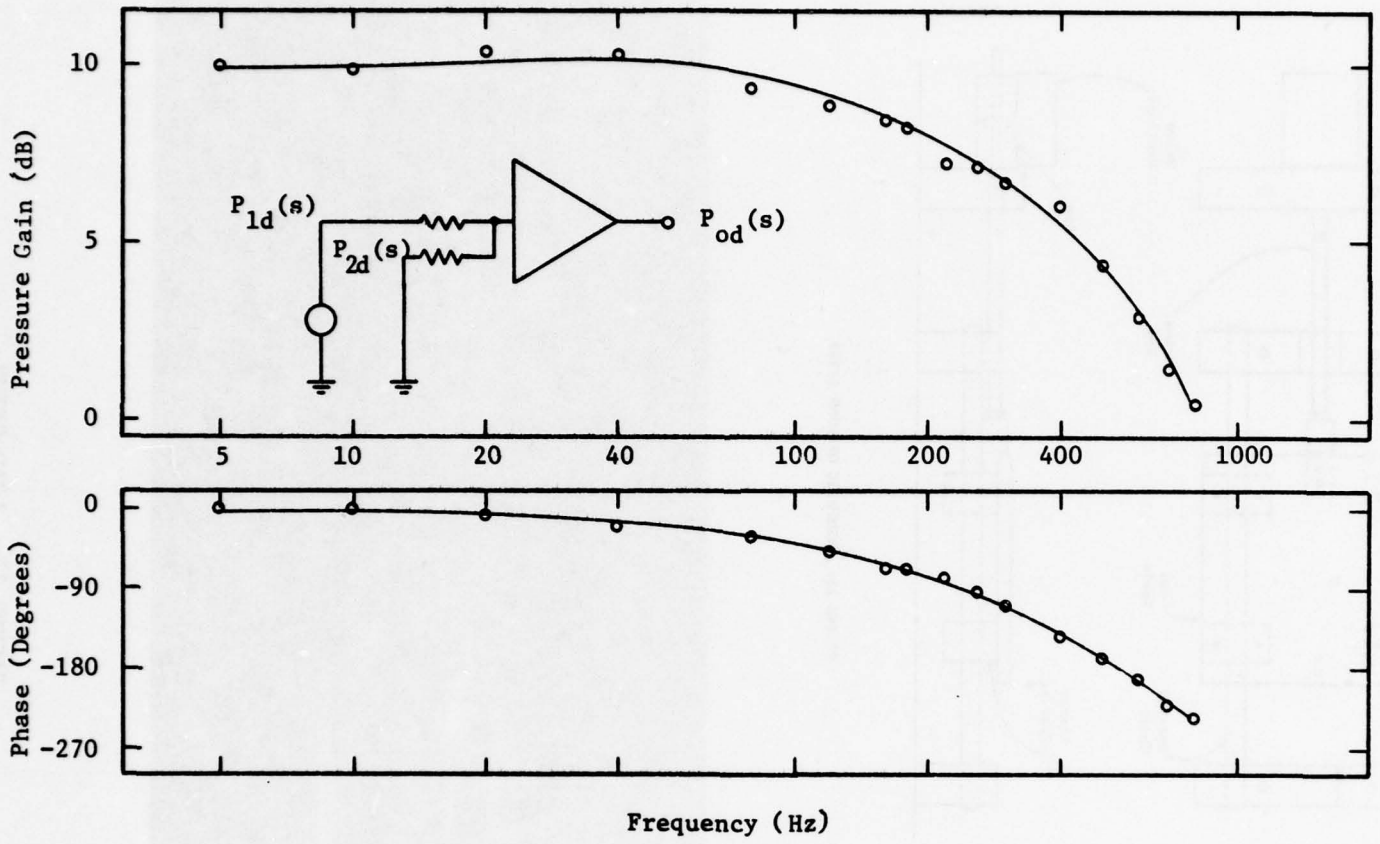

FIGURE 10: BLOCKED LOAD FREQUENCY RESPONSE OF SUMMING AMPLIFIER

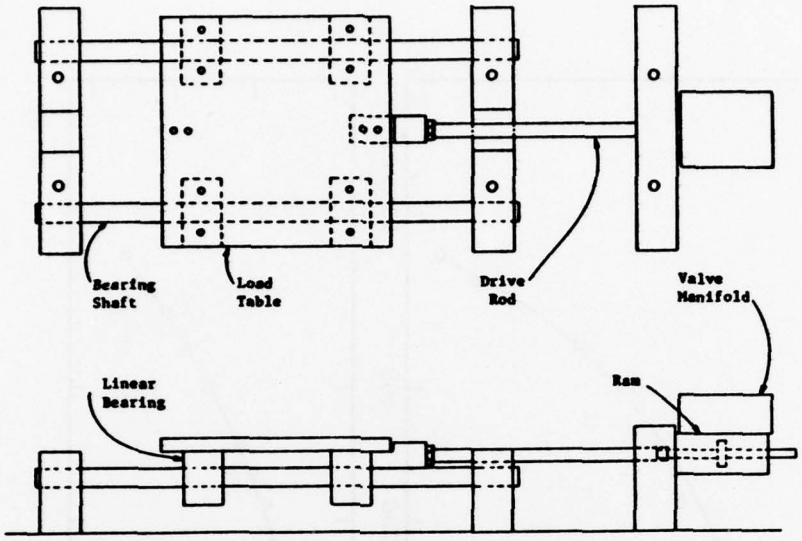

FIGURE 11: SCHEMATIC OF LOAD SETUP

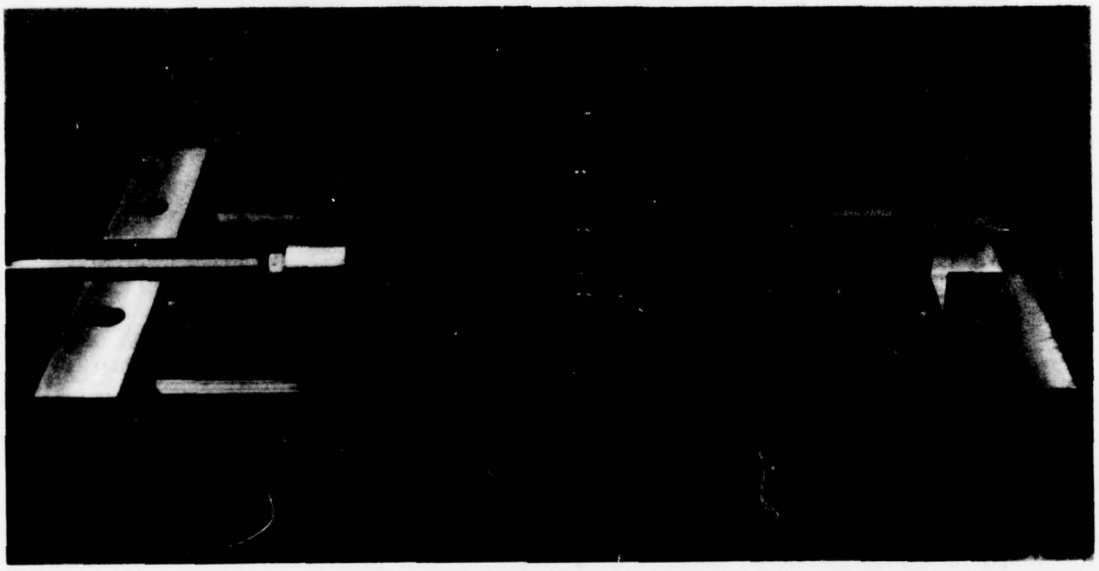

FIGURE 12: LOAD SETUP

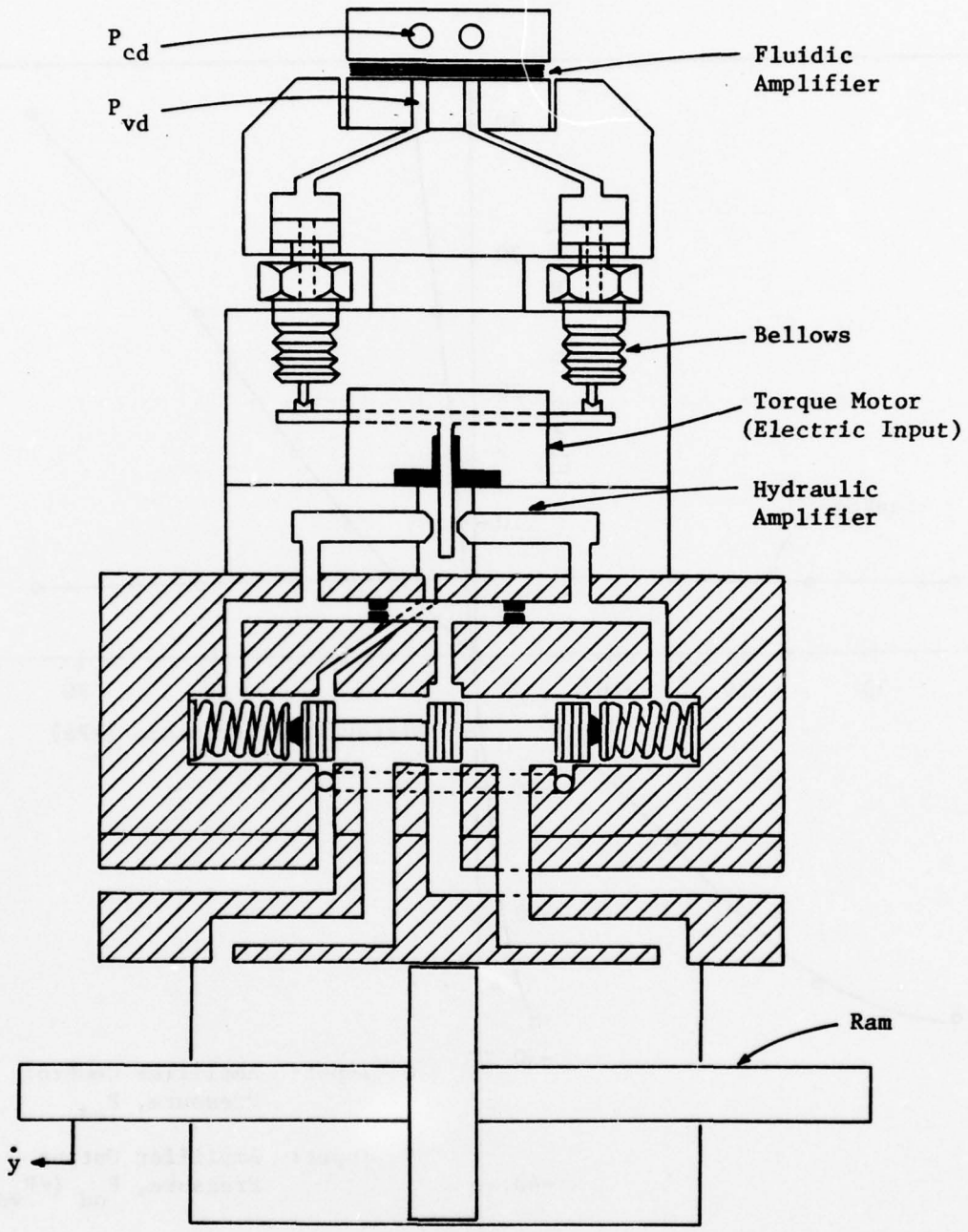

FIGURE 13: SCHEMATIC OF FLUID AND ELECTRICAL INPUT VALVE

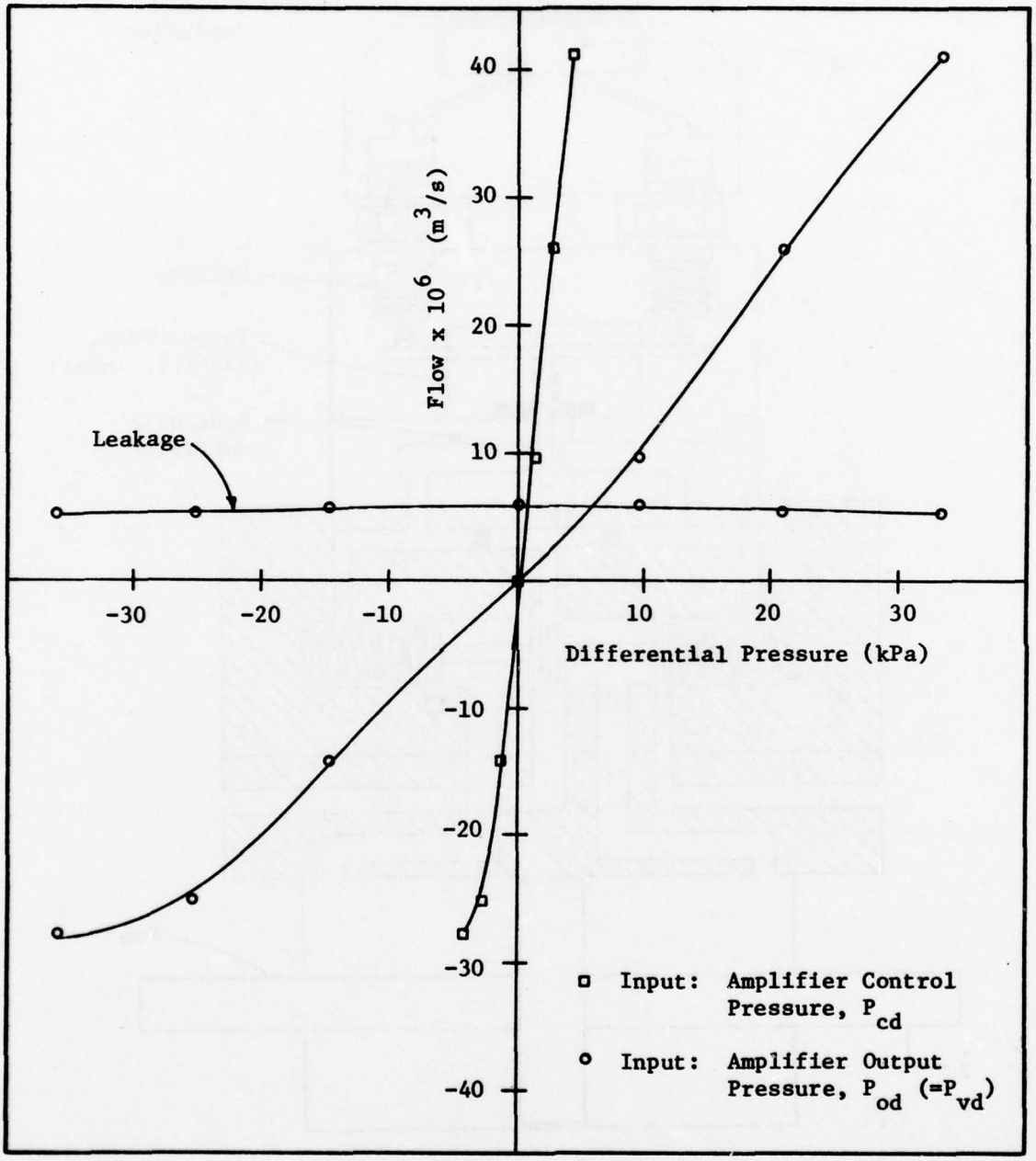

FIGURE 14: VALVE FLOW GAIN; FLUID INPUT

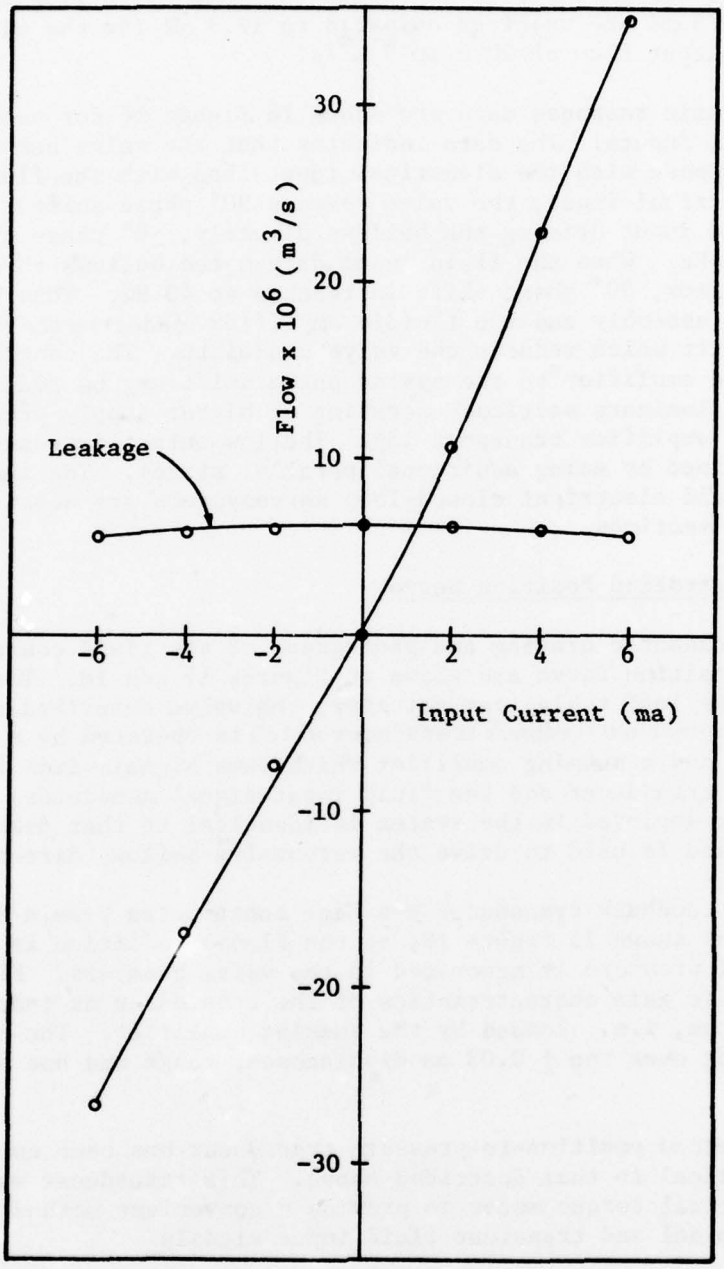

FIGURE 15: VALVE FLOW GAIN; ELECTRICAL INPUT

Input power requirements at the fluidic amplifier control ports of the fluid input valve are approximately an order of magnitude less than that for the electrical input valve to obtain the same valve flow rate. For the fluid case, 1.3 mW are required compared to 12.9 mW for the electrical case for an output flow of 20 x 10^{-6} m^3/s.

Dynamic response data are shown in figure 16 for both fluid and electrical inputs. The data indicates that the valve has a better frequency response with the electrical input than with the fluid input. With the electrical input, the valve reaches 90° phase shift at 82 Hz. With the fluid input driving the bellows directly, 90° phase shift is reached at 54 Hz. When the fluid input drives the bellows through the fluidic amplifier, 90° phase shift is reached at 40 Hz. Thus both the bellows drive assembly and the fluidic amplifier loaded by the bellows introduce phase shift which reduces the valve bandwidth. The contribution of the fluidic amplifier to the system phase shift may be reduced by using thinner laminate sections operating at higher supply pressures to reduce the amplifier transport lag. The low output impedance desired may be maintained by using additional parallel stages. The implementation of the fluid and electrical closed-loop servosystems are described in the following two sections.

3.2 Fluid Controlled Position Servo

A schematic drawing and photograph of the fluid controlled closed-loop position servo are shown in figures 17 and 18. The servo consists of the load table, ram actuator, the valve described above, a position-to-pressure feedback transducer which is operated by a linkage from the ram, and a summing amplifier which sums signals from the position feedback transducer and the fluid input signal generator. The summing amplifier employed in the system is identical to that described in Section 2 and is used to drive the servovalve bellows directly.

The feedback transducer has been constructed from a flapper-nozzle valve as shown in figure 19; as the flapper position is changed, a differential pressure is generated in the valve chambers. Figure 20 shows the static gain characteristics of the transducer as installed in the servo system, i.e., loaded by the summing amplifier. The characteristic is linear over the $\pm$ 0.03 mm displacement range and has a gain of 72 kPa/mm.

A second position-to-pressure transducer has been constructed which is identical to that described above. This transducer was mated with an electrical torque motor to provide a convenient method of generating sinusoidal and transient fluid input signals.

3.3 Electrohydraulic Position Servo

The electrohydraulic servo was constructed using a commercial electrical Direct Current Displacement Transducer (DCDT) for the feedback transducer, and a summing operational amplifier-servoamplifier to drive

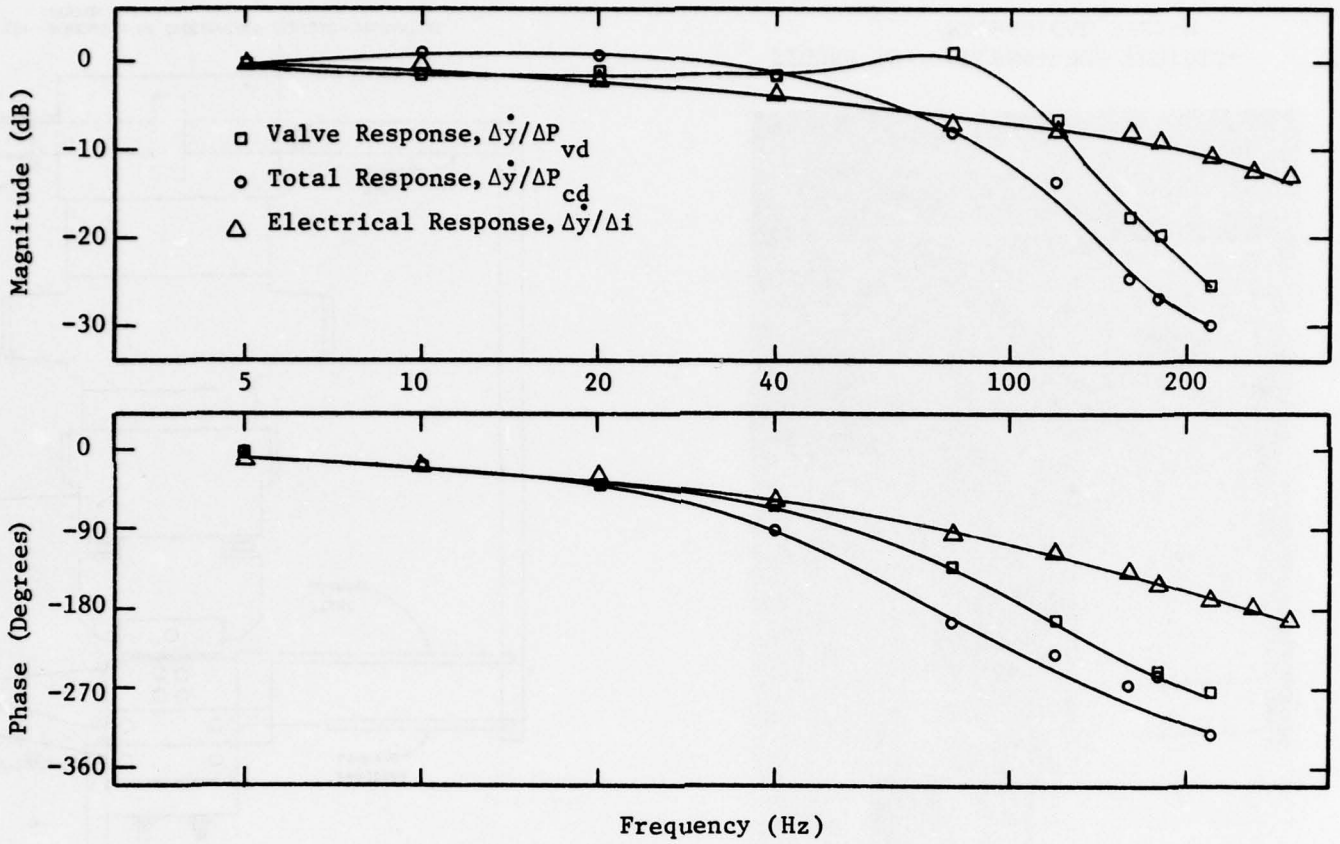

FIGURE 16: SERVOVALVE DYNAMIC RESPONSE

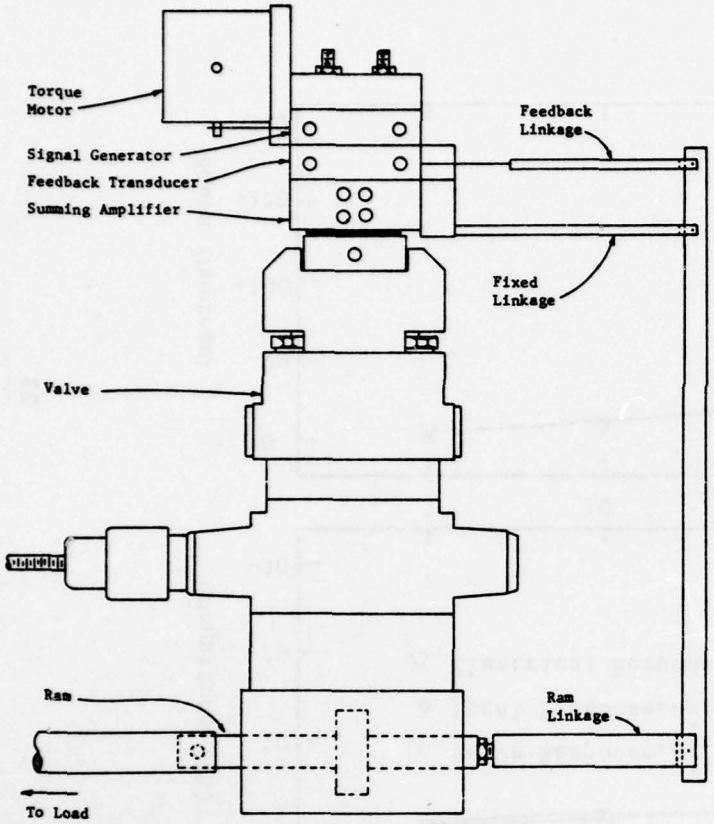

FIGURE 17: SCHEMATIC OF CLOSED-LOOP FLUIDIC - MECHANICAL SYSTEM

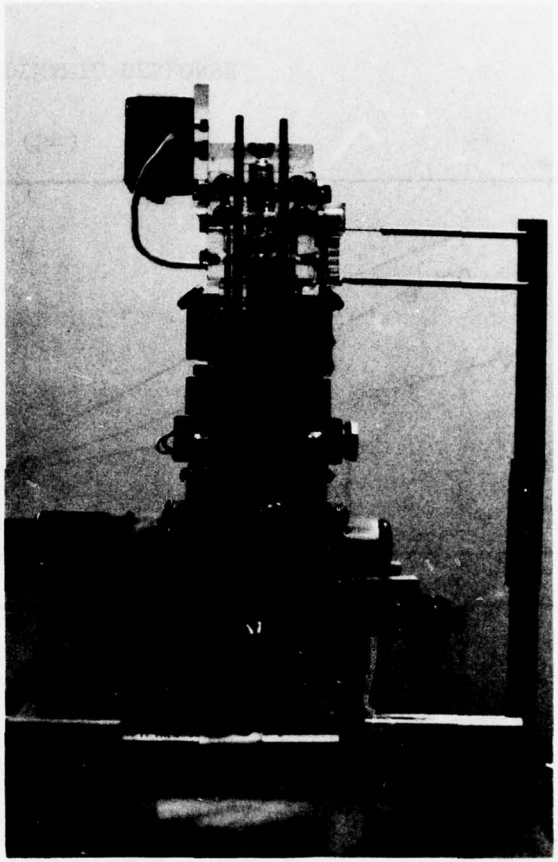

FIGURE 18: CLOSED-LOOP FLUIDIC-MECHANICAL SYSTEM

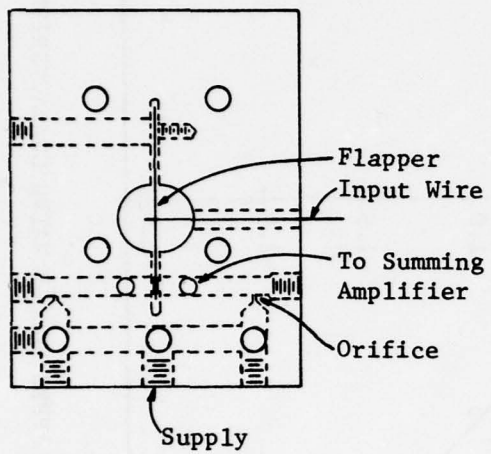

Scale 1:1

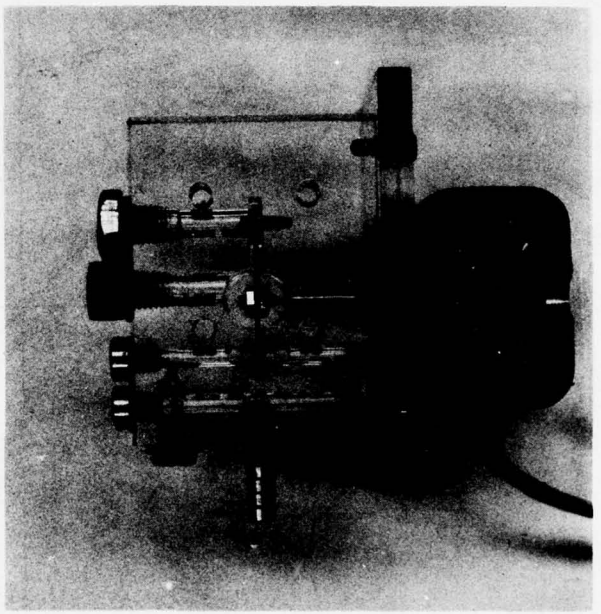

FIGURE 19: FLAPPER-NOZZLE VALVE SCHEMATIC AND PHOTOGRAPH

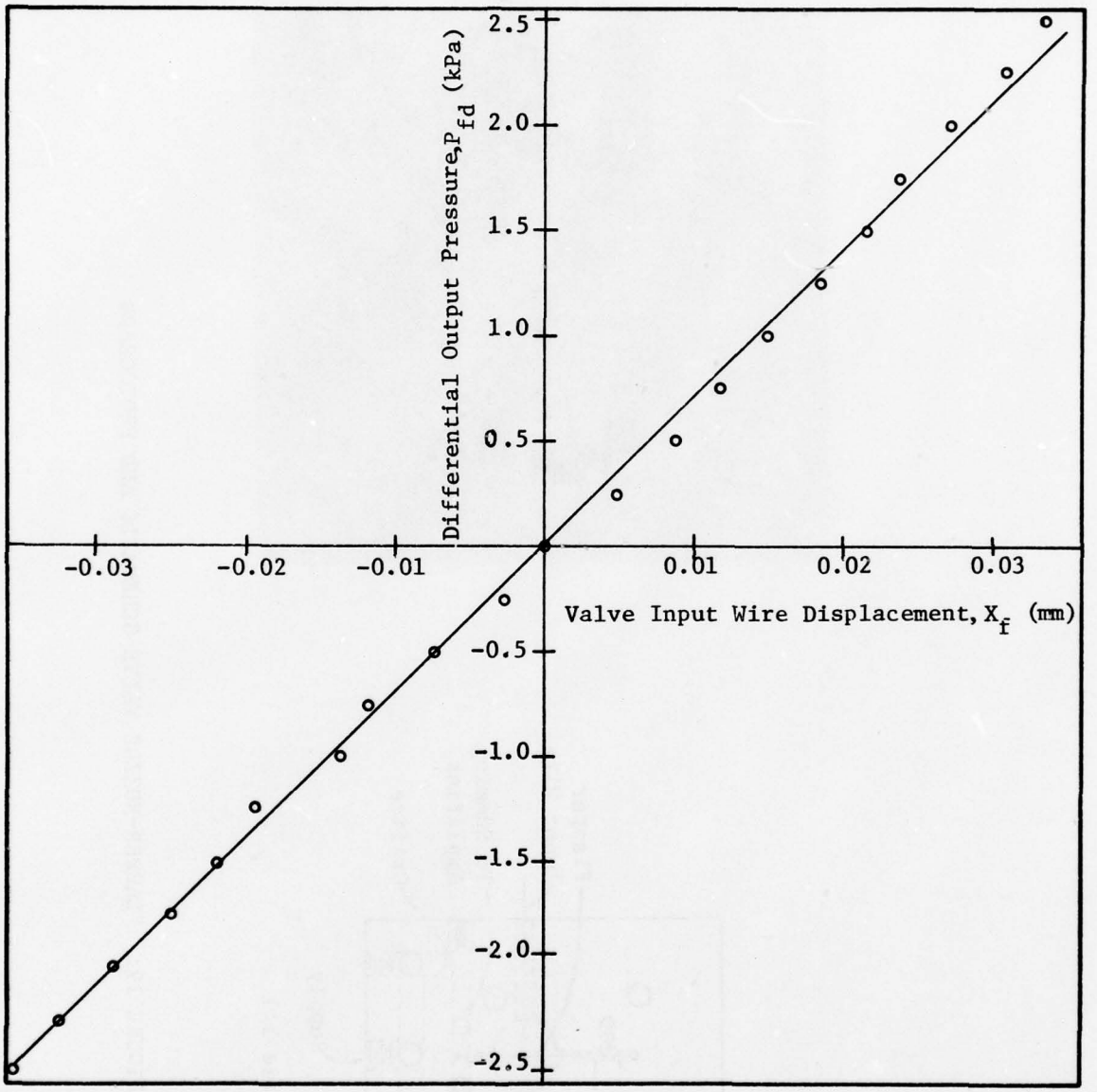

FIGURE 20: FLAPPER-NOZZLE VALVE CHARACTERISTICS

the torque motor in the first-stage of the servovalve.

3.4 Position Servosystem Linear Model Derivation

The elements of the fluid and electrical input position servos are summarized in block diagram form in figure 21. A linear model for the position servo has been derived as described below.

When the load carriage friction is represented as viscous, the sum of forces on the load mass yields

$$m\ddot{y} + b\dot{y} = P_L A_r - F_y, \tag{4}$$

where y = load position,

m = load mass,

b = viscous friction coefficient,

P_L = differential pressure across hydraulic ram,

A_r = ram area,

F_y = external load force,

$(\dot{}) = \frac{d}{dt}(\ )$.

For incremental motions of the ram from its center position, the actuator pressure-flow-velocity relationships may be derived as

$$Q_L = A_r\dot{y} + \frac{1}{2}\frac{V}{\beta}\dot{P}_L, \tag{5}$$

where Q_L = flow from valve to actuator,

V = actuator volume (single side),

β = fluid bulk modulus.

The ram is assumed to have no leakage.

For dynamic incremental, symmetric operation of the valve, over the frequency range from 0 to 120 Hz, the pressure-flow-input relationship may be represented in transfer function form as

$$Q_L = \frac{\omega_n^2}{s^2 + 2\xi\omega_n s + \omega_n^2} I - K_{pq} P_L, \tag{6}$$

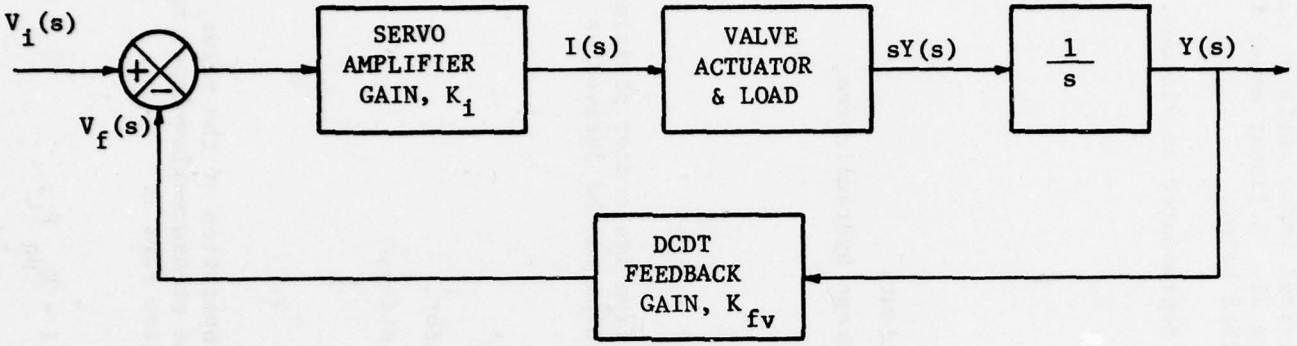

(a) Electromechanical System

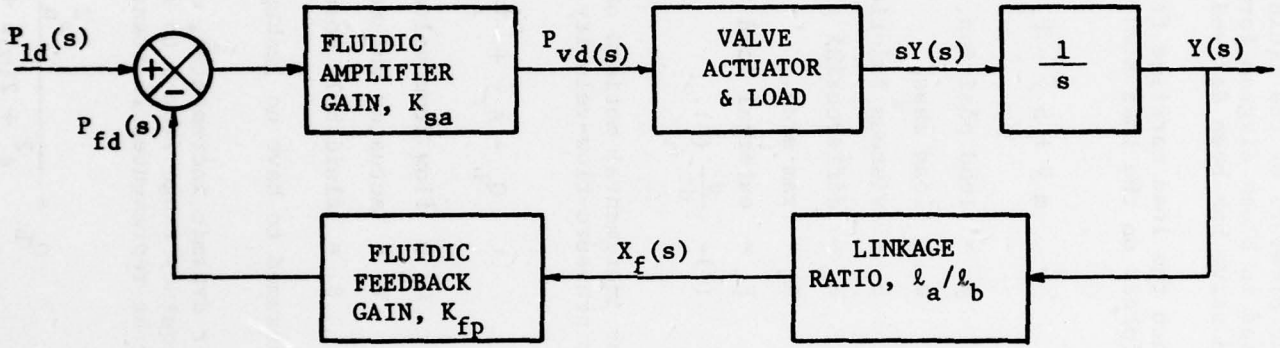

(b) Fluidic-Mechanical System

FIGURE 21: BLOCK DIAGRAM OF ELECTROMECHANICAL AND FLUIDIC-MECHANICAL SERVOSYSTEMS

where s = Laplace transform operator,

ξ = damping ratio,

ω_n = natural frequency,

K_{pq} = valve flow-load pressure gain,

I = input function.

For electrical inputs,

$$I = K_{qi}\, i, \tag{7}$$

where i = input current,

K_{qi} = valve flow-current gain.

For fluid inputs,

$$I = K_{qp} K e^{-\tau s} P_{cd}, \tag{8}$$

where P_{cd} = valve input pressure differential at amplifier control ports,

K_{qp} = valve flow-input pressure gain,

K = amplifier blocked load gain,

τ = delay time.

The valve representation in equation (6) is derived from a fit of the valve dynamic frequency response over the range from 0 to 120 Hz. The additional phase lag introduced in the fluidic input valve by both the fluid amplifier and the bellows is represented by the term $e^{-\tau s}$ in equation (8). Figure 22 shows agreement between the representations of equations (6) - (7) and (6) - (8) with experimental data, assuming no load conditions. The fit with experimental data is good over the 0 to 120 Hz frequency range with the following parameter values.

$$\omega_n = 503 \text{ rad/s}$$
$$\xi = 1.0$$
$$\tau = 2.7 \times 10^{-3} \text{s}$$

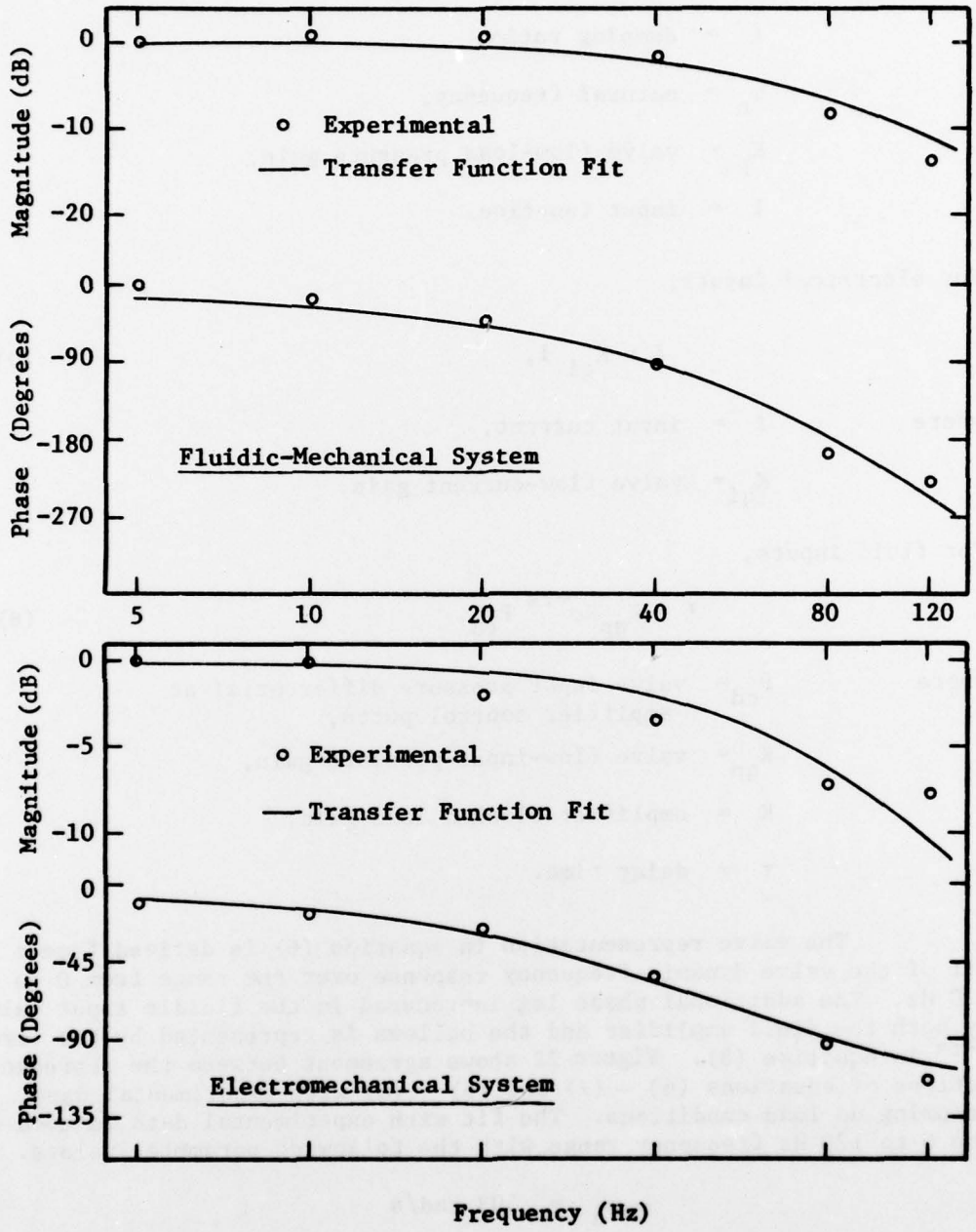

FIGURE 22: COMPARISON OF EXPERIMENTAL DATA WITH ANALYTICAL APPROXIMATION FOR VALVE DYNAMIC RESPONSE

The electrical controller and feedback transducer implemented with commercial equipment may be described as

$$i = K_i(V_i - V_f) = K_i(V_i - K_{fv}y), \tag{9}$$

where
V_i = input voltage,
V_f = feedback voltage,
K_{fv} = voltage-position feedback transducer gain,
K_i = servo amplifier gain.

The fluid controller and feedback transducer may be described as

$$P_{cd} = P_{vd}/K = K_{sa}(P_{ld}-P_{fd})/K = K_{sa}(P_{ld}-K_{fp}(\ell_a/\ell_b)y)/K, \tag{10}$$

where
K_{sa} = fluid summing amplifier static gain,
P_{ld} = input pressure differential,
P_{fd} = feedback pressure differential,
P_{vd} = valve input pressure differential at bellows,
K_{fp} = pressure-position feedback transducer gain,
ℓ_a/ℓ_b = linkage ratio,
ℓ_a = feedback pivot to fixed pivot distance,
ℓ_b = ram pivot to fixed pviot distance.

The equations listed above represent simple, linear models for the fluid and electrical input closed-loop position servos. The parameters defined in these equations are listed in table I, with numerical values for the servo components obtained from either measurement of individual element characteristics or manufacturer calibrations.

The equations describing the two closed-loop models were solved for a step input in command position as shown in figure 23 for three values of loop gain. The nominal loop gain for each system was selected to yield the minimum system rise time while keeping response overshoot to less than 5 %. Then responses were computed for double and half the value of nominal gain. For double the value of gain, the response time decreases and the overshoot exceeds 25% in both systems, while with half the gain, the response time increases by almost a factor of two and no overshoot occurs. The nominal open-loop gains for the two systems are

TABLE I: SERVOSYSTEM PARAMETERS

ACTUATOR		
Area, A	432 mm^2	0.67 in^2
Volume (single side), V	8.19×10^3 mm^3	0.5 in^3
Oil bulk modulus, β	1.38×10^6 kPa	2×10^5 psi
VALVE		
Natural frequency, ω_n (electrical input 90° phase shift frequency)	503 rad/s	
Damping ratio, ξ (electrical input)	1.0	
Flow gain, K_{qi} (electrical input)	4.99×10^3 $mm^3/s/mA$	0.305 $in^3/s/mA$
Load pressure gain, K_{pq}	0.177 $mm^3/s/kPa$	7.46×10^{-5} $in^3/s/psi$
Flow gain, K_{qp} (pressure input at bellows)	1.22×10^3 $mm^3/s/kPa$	0.513 $in^3/s/psi$
Transport lag, T (fluid system)	2.7×10^{-3} s	
LOAD		
Mass, m	16.64 kg	0.095 lb-s^2/in
Damping constant, b	29.6 N/m/s	0.169 lb/in/s
CONTROLLER; ELECTRICAL		
Servoamplifier gain, K_i	40.0 mA/V	
Feedback gain, K_{fv}	0.26 V/mm	6.6 V/in
CONTROLLER; FLUIDIC		
Fluid summing amplifier gain, K_{sa}	3.0	
Feedback gain, K_{fp} (flapper nozzle valve)	71.6 kPa/mm	264 psid/in
Feedback linkage ratio, ℓ_a/ℓ_b	20.57/181.53 mm/mm	0.81/7.147 in/in

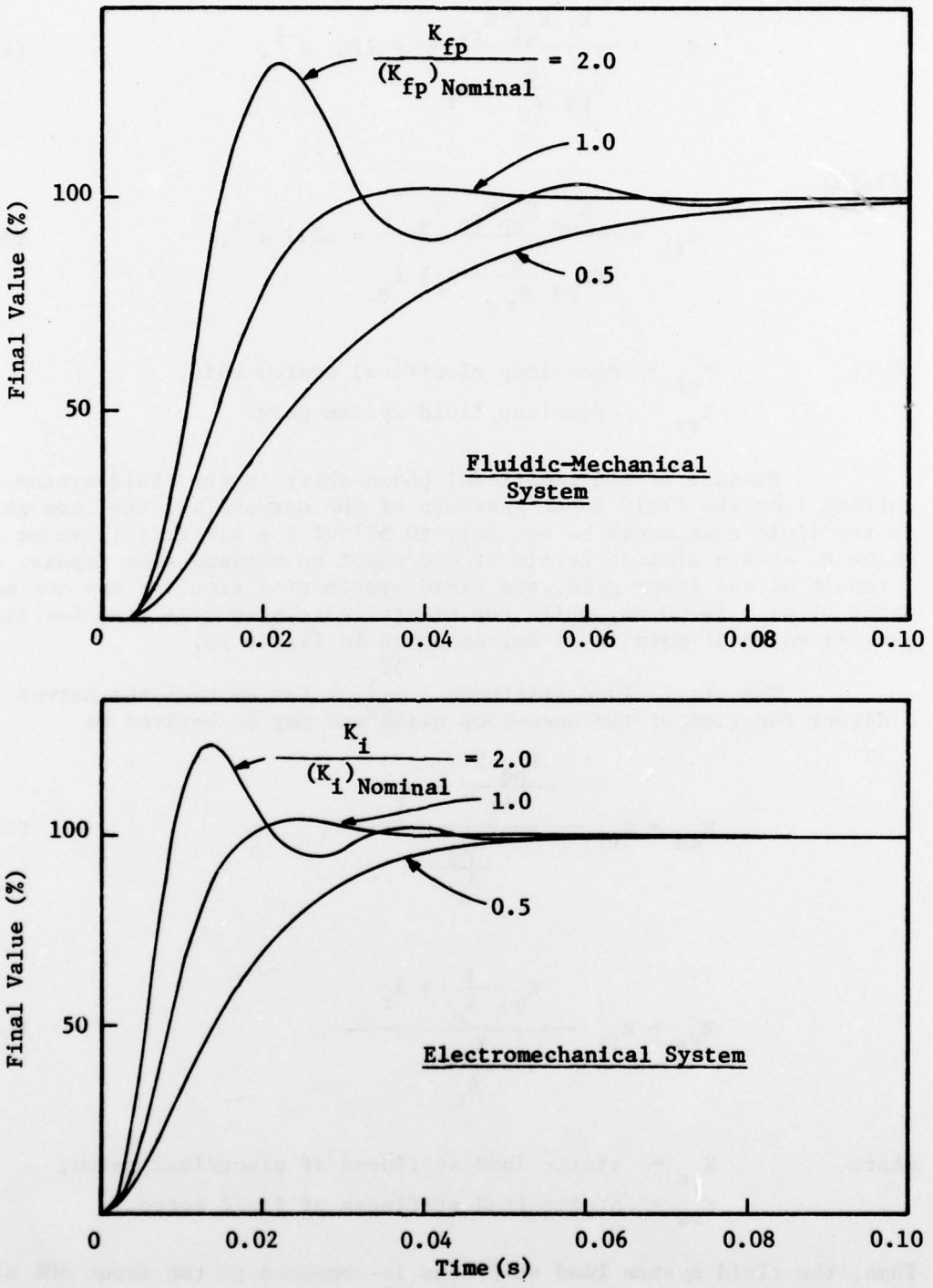

FIGURE 23: COMPUTED STEP RESPONSES OF CLOSED-LOOP POSITION SERVOSYSTEMS FOR SELECTED VALUES OF GAIN

(electrical)

$$K_{e\ell} = \frac{K_i K_{qi} K_{fv}}{K_{pq} \frac{b}{A_r} + A_r} = 120 \ s^{-1}, \tag{11}$$

(fluid)

$$K_{f\ell} = \frac{K_{sa} K_{qp} K_{fp} \ell_a}{(K_{pq} \frac{b}{A_r} + A_r) \ell_b} = 68.7 \ s^{-1}, \tag{12}$$

where $K_{e\ell}$ = open-loop electrical system gain,

$K_{f\ell}$ = open-loop fluid system gain.

Because of the additional phase shift in the fluid system resulting from the fluid input elements of the servovalve, the loop gain in the fluid system can be set only to 57% of the electrical system value to obtain similar levels of overshoot to command step inputs. As a result of the lower gain, the fluid system rise time for the nominal value of gain is 30 ms, while the electrical system rise time for its nominal value of gain is 18 ms, as shown in figure 23.

The static load stiffness ($\frac{\Delta F_y}{\Delta y}$) for each of the servos is a direct function of the open-loop gains and may be derived as

$$K_{es} = K_{e\ell} \frac{\frac{K_{pq} b}{A_r} + A_r}{\frac{K_{pq}}{A_r}}, \tag{13}$$

$$K_{fs} = K_{f\ell} \frac{K_{pq} \frac{b}{A_r} + A_r}{\frac{K_{pq}}{A_r}}, \tag{14}$$

where K_{es} = static load stiffness of electrical servo,

K_{fs} = static load stiffness of fluid servo.

Thus, the fluid system load stiffness is computed to the about 60% of the electrical system load stiffness.

3.5 Measured Servo Responses

The fluid and the electrical input servosystems described above were tested with the nominal values of gain given in table I. Measured static load stiffness data are summarized in figure 24. The stiffness for the electrical system is 8.8×10^3 N/mm and for the fluid system is 6.7×10^3 N/mm. The measured fluid system load stiffness is 75 % of the corresponding electrical system load stiffness because of its lower loop gain.

The responses of the two systems to a position command input of 0.3 mm is shown in the oscilloscope photographs of figure 25. The experimentally measured responses illustrate essentially no overshoot with the approximate response times of the fluid and electrical servos respectively 38 and 23 ms. A comparison of these experimentally measured responses to the computed responses is contained in figure 26. This comparison shows that for both systems, the computed responses have faster rise times and more overshoot than the experimental responses; however, the computed and experimentally measured responses are in relatively good agreement.

Both the analytical and experimental data have shown that to achieve equivalent levels of overshoot in response to a position command, the loop gain of the fluid input system is limited to about 57% of that of the electrical input system. As a result of this reduced gain, the fluid input system response time is increased and the load stiffness is decreased when compared to that of the electrical input system. The primary factor contributing to the reduction in allowable fluid input system gain while maintaining a response with no overshoot, is the greater response time of the fluidic amplifier and bellows drive assembly than that of the torque motor drive. As described above, the fluidic amplifier can be designed to reduce its response time. In addition, the bellows and first-stage flapper-nozzle valve may be eliminated so that the spool is driven directly by a fluidic amplifier. This type of system offers the potential of a fluid input valve with response times comparable to the electrical input valve.

4. SUMMARY AND CONCLUSIONS

This study has resulted in the development and performance testing of hydraulic fluid summing and proportional gain amplifiers for use in closed-loop position servosystems. The amplifiers developed use HDL 311005 laminates which have improved frequency response and input impedance characteristics compared to previous laminates tested. The summing amplifier constructed from the 311005 laminates and drilled laminar flow resistances has a frequency response which decreases by 3 dB and reaches 90° phase shift at 240 Hz.

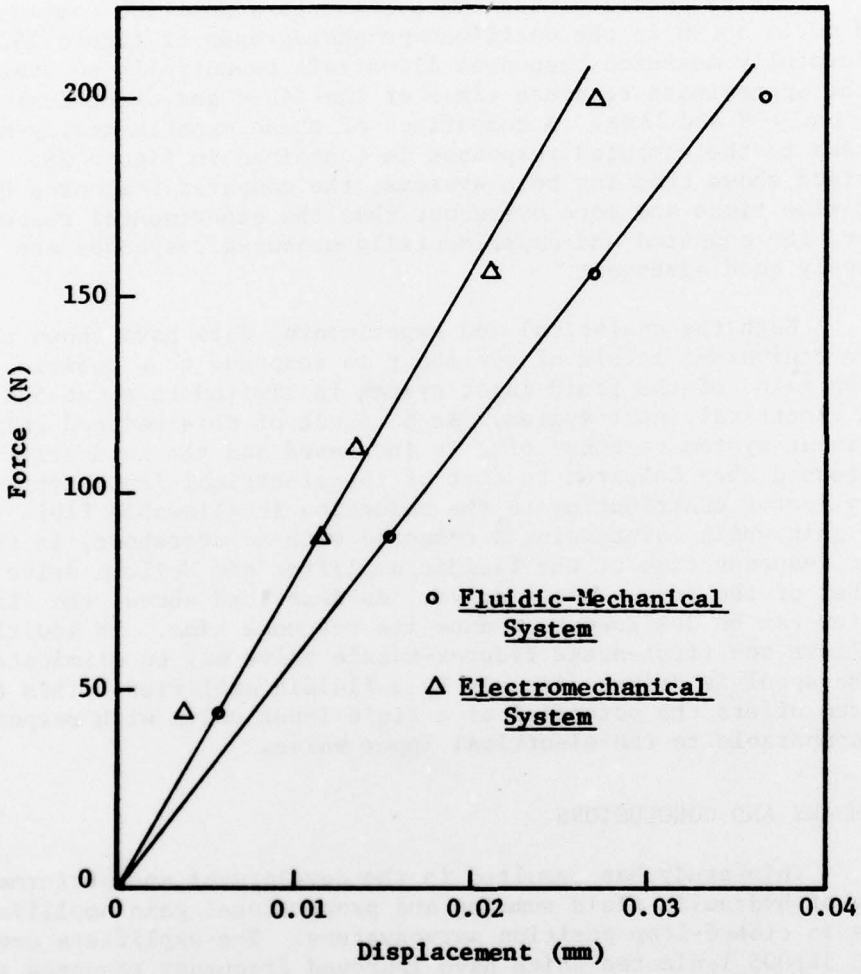

FIGURE 24: STATIC LOAD STIFFNESS OF THE EXPERIMENTAL SERVOSYSTEMS

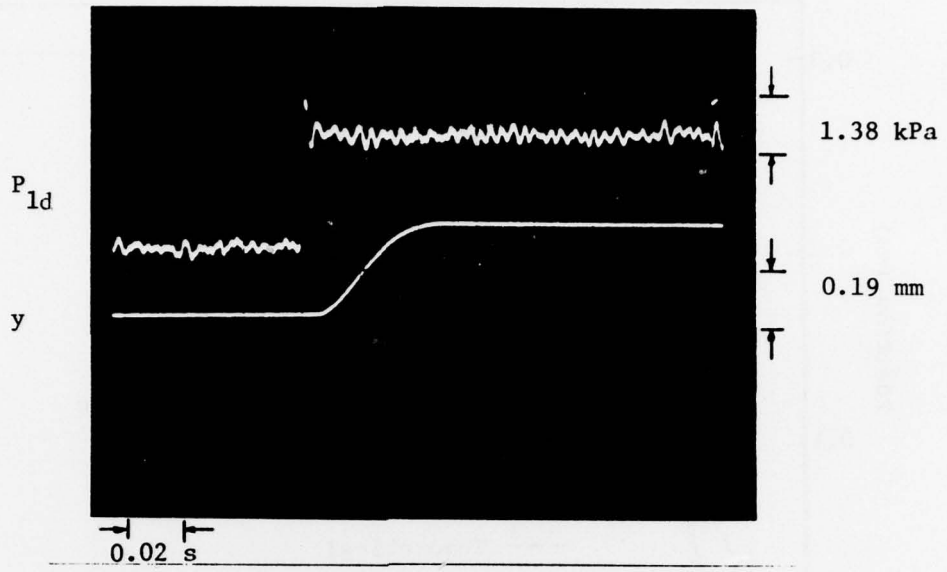

Fluidic-Mechanical System

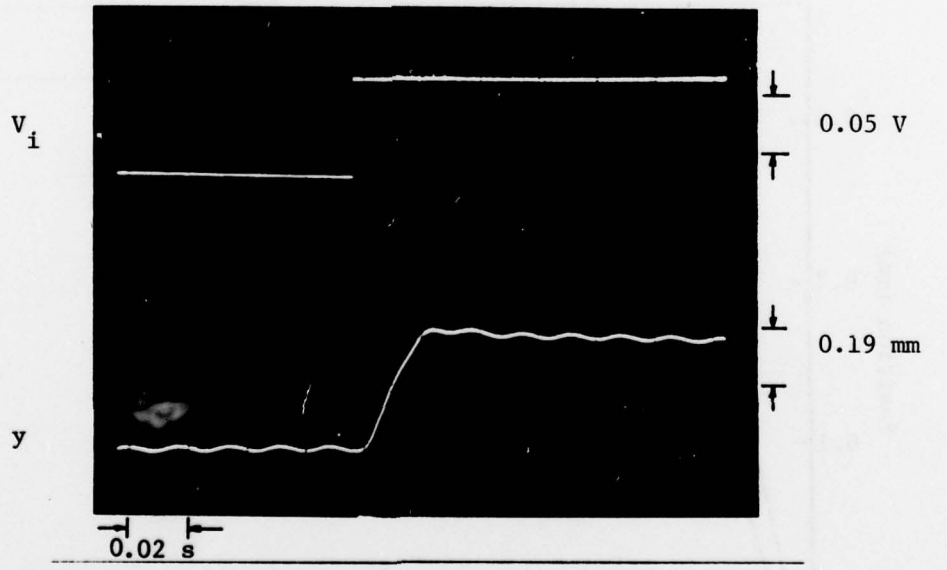

Electromechanical System

FIGURE 25: MEASURED SERVOSYSTEM STEP RESPONSES

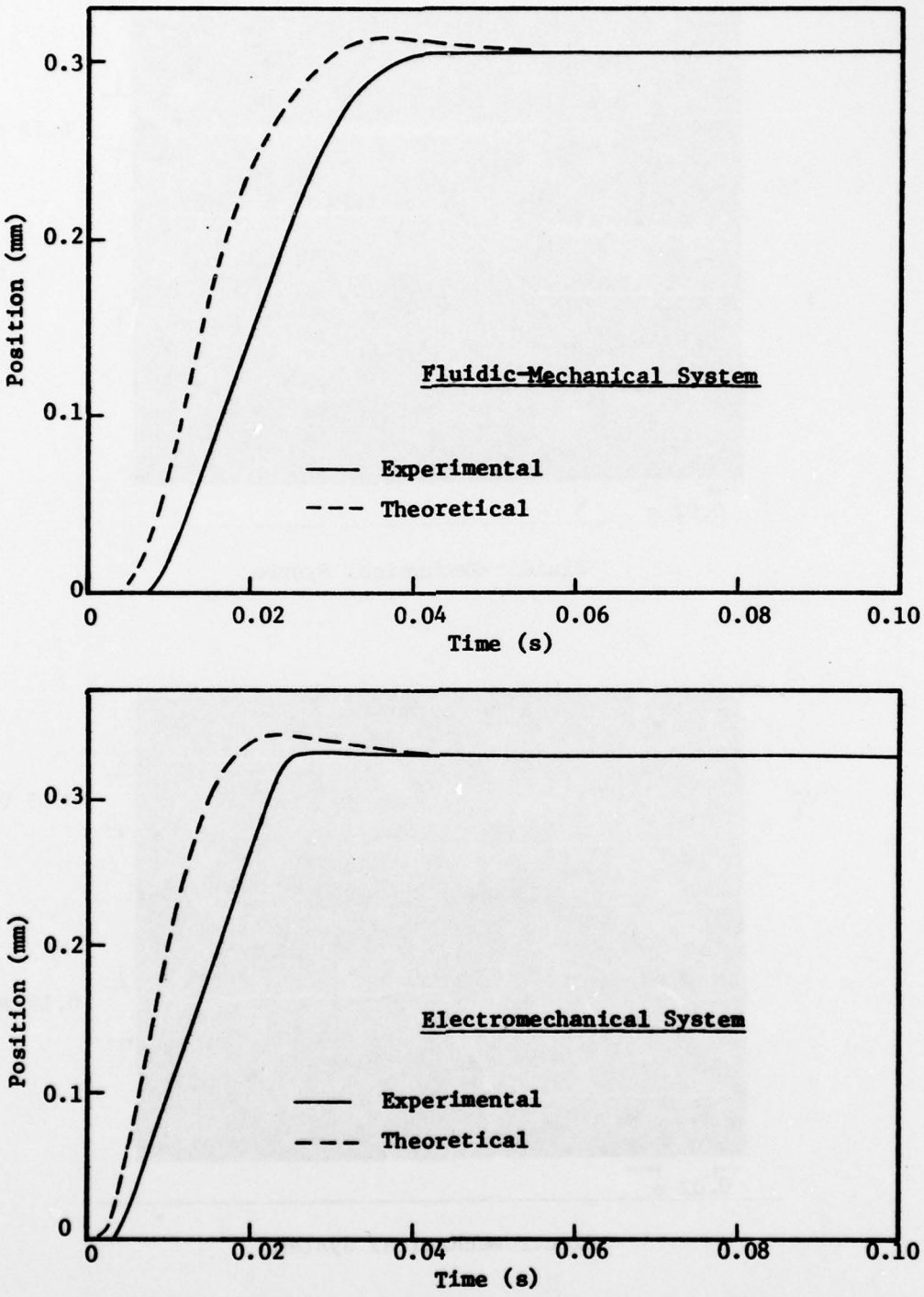

FIGURE 26: COMPARISON OF EXPERIMENTAL AND THEORETICAL SERVO-SYSTEM STEP RESPONSES

A closed-loop position control servo has been constructed using the summing amplifier, a fluid input servovalve, hydraulic ram, mass load, and position-to-fluid feedback transducer. The servosystem exhibits a command step response time of 38 ms and has a load stiffness of 6.7×10^3 N/mm. Comparison of the fluid servosystem with its direct electrical counterpart has shown that system response is limited primarily by the fluid input servovalve. This valve consists of two-stages; a flapper-nozzle valve first-stage and a spring centered spool second-stage, augmented by a fluidic amplifier driving a pair of bellows which positions the flapper. This implementation method results in a valve which has a lower dynamic response capability than its electrical counterpart, which employs a torque motor to position the flapper. The valve frequency response data shows that 90° phase shift is reached by the fluid input system at 40 Hz and by the electric input system at 82 Hz. This lower dynamic response capability of the fluid input valve results in a smaller usable gain than that of the electric input valve in a closed-loop position servo for equivalent levels of closed-loop step response overshoot; the end result is both decreased closed-loop dynamic response capability and load stiffness.

The specific data measured on both the fluid and electrical servos, as well as supporting analysis, have shown the need to develop fluid input servovalves which have response characteristics comparable to electrical input valves if comparable closed-loop servo performance is to be obtained. One of the goals in the next phase of this research project on high performance hydraulic control systems is the development of a fluid input servovalve with improved dynamic response characteristics. A valve consisting of a fluidic amplifier first-stage directly driving a spool second-stage will be evaluated in the initial part of this research effort.

APPENDIX A. -- NOMENCLATURE

A_r	ram area (mm^2)
b	viscous friction coefficient (nt/m/s)
b_s	supply nozzle width (mm)
d	diameter of resistor (mm)
F_y	external load force (N)
h	laminate thickness (mm)
i,I(s)	input current (ma)
I	input function
K	amplifier blocked load gain
$K_{e\ell}$	electromechanical system open loop gain
K_{es}	electromechanical system static load stiffness (N/mm)
$K_{f\ell}$	fluidic-mechanical system open loop gain
K_{fp}	pressure-position feedback transducer gain (kPa/mm)
K_{fs}	fluidic-mechanical system static load stiffness (N/mm)
K_{fv}	voltage-position feedback transducer gain (V/mm)
K_i	servoamplifier gain (ma/V)
K_{pq}	valve flow-load pressure gain (mm^3/s/kPa)
K_{qi}	valve flow-current gain (mm^3/s/ma)
K_{qp}	valve flow-input pressure gain (mm^3/s/kPa)
K_{sa}	fluid summing amplifier static gain
ℓ	length of resistor (mm)
ℓ_a	feedback pivot to fixed pivot distance (mm)
ℓ_b	ram pivot to fixed pivot distance (mm)
m	load mass (kg)
N_R	Reynolds Number
N_R'	modified Reynolds number
P_c	control port pressure (kPa)
P_{cd}	control port pressure differential (kPa)
P_{co}	control port bias pressure ($(P_{c\ell} + P_{cr})/2$) (kPa)
P_{fd}	feedback pressure differential (kPa)
P_L	differential pressure across hydraulic ram (kPa)

P_{od}	output port pressure differential (kPa)
P_{vd}	valve input pressure differential (kPa)
P_s	supply pressure (kPa)
P_{1d}, P_{2d}	summing amplifier input pressure differential (kPa)
Q_c	control port flow (m^3/s)
Q_L	flow from valve to actuator (m^3/s)
Q_s	power jet supply flow (m^3/s)
R_i	amplifier input impedance ($N\text{-}s/m^5$)
R_1, R_2	resistors ($N\text{-}s/m^5$)
R'	resistance as defined in eq. (3)
s	Laplace transform operator
V	actuator volume (mm^3)
V_f	feedback voltage (V)
V_i	input voltage (V)
$x_f, X_f(s)$	flapper nozzle valve input wire displacement (mm)
x_{th}	supply nozzle throat length (mm)
$y, Y(s)$	load position (m)
β	fluid bulk modulus (kPa)
$\Delta( )$	increment or difference of a quantity ( )
μ	absolute viscosity ($N\text{-}s/m^2$)
ξ	second-order factor damping ratio
ρ	fluid density (kg/m^3)
σ	amplifier power nozzle aspect ratio [h/b_s]
τ	delay time constant (s)
ω_n	second-order factor natural frequency (rad/s)
$(\dot{})$	time derivative

SUBSCRIPTS

ℓ	left
r	right

Fluidics Distribution List

Defense Documentation Center
Cameron Station, Building 5
Alexandria, Va. 22314
ATTN: DDC-TO ~~20~~ 12 copies

Commander HDL
2800 Powder Mill Road
Adelphi, Md. 20783 6 copies